## Supplemental Text 1. Analysis of Radiocarbon Dates

Our analysis of radiocarbon dates consists of two components: (1) the identification of problematic dates, which we exclude from subsequent analyses and chronology-building; and (2) the application of Bayesian statistics to refine remaining valid dates. We should emphasize that the former is the most important part of chronology-building. The results of Bayesian analysis also depend on the effective detection of questionable dates.

### *Identification of Problematic Dates*

The process of eliminating problematic radiocarbon dates is called chronometric hygiene by some scholars (Fitzpatrick 2006; Nolan 2012; Spriggs 1989; Taché and Hart 2013). Scholars have suggested various criteria for identifying questionable dates, which are roughly classified into the domains of chronometric issues and archaeological interpretation (Blockley and Pinhasi 2011; Collett and Robertshaw 1983; Inomata et al. 2013; Pettitt et al. 2003; Telford et al. 2004; Waterbolk 1971). The former concerns measurement errors, sample contamination, pretreatments, reservoir effects, and other issues that are dealt with primarily at radiocarbon dating laboratories. The latter includes the association of samples with cultural features, stratigraphic integrity, sample taphonomy, and agreement with ceramic phases, all of which need to be evaluated before samples are sent to labs and after lab results are received. The old wood problem, or the difference between the growth date of dated plant material and its final deposition date, crosscuts the two domains. We should note that many studies on chronometric hygiene concern issues of Paleolithic or Neolithic periods, initial colonization, and other cases of early occupation (e.g., Hunt and Lipo 2006; Waters and Stafford 2007; Wilmshurst et al. 2011). Our study builds on these earlier efforts, but we tailor our approach specifically to the nature of our data set and for the archaeological settings of Kaminaljuyú and southern Mesoamerica, which are characterized by densely aggregated settlements, large buildings, and long continuous occupation.

The most serious problem for radiocarbon dating in southern Mesoamerica, as we perceive it, is the redeposition of old charcoal resulting from long continuous occupation in the same locations and frequent rebuilding using old fill materials (Pendergast 2000). This problem is further compounded by old wood problems, which derive from the use of large tropical trees, the presence of durable buildings that stood for many years, and the long use lives of some wooden objects that may have been passed down through generations as heirlooms. The use of annual or short-lived species or parts—such as maize grains and seeds—for radiocarbon dating would avoid the old wood problem, but we still need to consider the possibility of redeposition for these materials. Human and animal skeletal materials from secure contexts may eliminate both the stratigraphic mixing and old wood problems, but marine and freshwater reservoir effects may make their radiocarbon measurements substantially older than their true ages unless their diets consisted exclusively of terrestrial materials (Culleton 2006; Keaveney and Reimer 2012). Given these factors, when problematic radiocarbon dates are not eliminated, resulting chronologies tend to be older than they should be. Redeposited charcoal and old wood are not evident at the time of excavation. Their detection needs to rely largely on comparison among multiple radiocarbon dates after lab results are received. All of the samples examined in our study are charcoal, and none are described as annual or short-lived species or parts. Therefore, the evaluation of the validity of each sample is critical.

*Chronometric Criteria.* The reliability of radiocarbon measurements has improved significantly over the years. Some scholars recommend that dates measured before 1970 and those with large error ranges be categorically excluded (Pettitt et al. 2003; Taché and Hart 2013). In examining the chronologies of Ceibal and the Olmec area, Inomata et al. (2013) used 1980 as a cut-off year. In the present study, our approach is more inclusive. We include all available radiocarbon dates in our initial evaluation for several reasons. First, whereas studies examining initial colonization or the Paleolithic and Neolithic periods in other parts of the world typically deal with data that is loosely replicable through the excavation of additional sites, the archaeology of Kaminaljuyú demands that researchers respect a greater degree of historical uniqueness of individual features and buildings. It may not be possible to re-excavate important features investigated in early days, and datable materials from such remains may not be available anymore. Old radiocarbon measurements on those features should not be dismissed easily. Dates associated with the Mound E-III-3 tombs are good examples.

Second, the number of radiocarbon dates associated with Kaminaljuyú that were recently measured with accelerator mass spectrometry (AMS) is still small. Third, in the conditions of Kaminaljuyú and the southern Maya area, redeposited charcoal may introduce larger and more frequent error than might be caused by chronometric inaccuracies. In such cases, our priority is to increase the reliability of our identification of valid dates by including a larger number of radiocarbon measures. In addition, although AMS is generally more accurate and precise than the earlier beta-counting method, the use of smaller samples for AMS may have increased the chance of including redeposited old charcoal. Larger chunks of charcoal used for conventional dating were less likely to be redeposited materials (Lanting and van der Plicht 1994; Pendergast 2000). Fourth, the difference between the Shook-Hatch chronology and our revised one is as large as 300 years. For the evaluation of such highly discrepant chronologies, even radiocarbon measurements from early days present sufficient utility. We should emphasize that our chronology relies primarily on recently obtained measurements, and older assays are used as supplementary data. This also means that the current database of radiocarbon measurements on Kaminaljuyú is far from ideal, and its chronology needs to be revised and refined with new data in the future.

The publications containing dates related to Kaminaljuyú do not report specific information that would aid with the evaluation of chronometric issues, such as C/N ratios, $\delta^{13}C$, sample weights, dated plant species, and specific pretreatments used. Thus, most of the chronometric issues and old wood problems, along with the question of redeposited charcoal, need to be evaluated through comparison of multiple dates. The only set of invalid dates that can be confidently excluded due to chronometric problems is the one from the Carnegie Project, which was processed by the University of Chicago lab in the 1950s (see main article text).

*Archaeological Criteria.* Stratigraphic mixing is common at a site like Kaminaljuyú with an extremely long history of occupation. Old charcoal and other materials were frequently reincorporated in later deposits. At the same time, younger materials may have been introduced in older deposits through animal burrows, root action, postholes, and inadequate excavation. Thus, stratigraphic mixing in both directions is possible, but we assume that at most sites in southern Mesoamerica the mixing of older materials in a deposit is substantially more prevalent than the mixing of younger ones. Just consider the chronological placement of ceramic sherds included in a deposit. The occurrence of ceramics of earlier periods in a given deposit is fairly common; ceramics of later periods can be present, but they are usually far less frequent.

In the evaluation of radiocarbon dates (and in the collection of samples for dating), we need to consider the nature of deposits. We can rank the types of deposit in order of desirability for radiocarbon dating. The optimum type includes primary deposits that contain no or little soil, such as charcoal contained in stucco and dense carbon deposits associated with in situ burning events or hearths. Chances of stratigraphic mixing in these cases are small. Annual or short-lived species or parts obtained from such deposits represent the best possibility for good radiocarbon dating. In situ building materials, such as a post found in its posthole, are also stratigraphically secure, but we still need to consider the old wood problem, including the recycling of building materials from earlier structures. The next best context may be primary deposits associated with discrete depositional events, such as burials and caches. However, as long as they contain soils, we need to consider the possibility that these soils already included old charcoal before their deposition. In addition, wood objects deposited in such contexts may have had long use life. Primarily deposited human and animal skeletal materials in such contexts eliminate the issues of redeposition and old wood, but marine and freshwater reservoir effects may affect their radiocarbon measurements unless they are terrestrial-feeding species. Other primary deposits, such as middens and on-floor materials, also present good possibilities, but thick middens reflecting long depositional periods are more likely to contain older materials. Mixed deposits, typically construction fill, are least desirable, but transposed middens and dumps containing materials transferred from short-period primary deposits present certain utility for radiocarbon dating.

*Specific Approaches.* Most of the problems mentioned, including various chronometric issues, redeposition of older materials, stratigraphic mixing, and old wood, are not apparent at the time of excavation or in published information. Problematic dates need to be identified through the examination of consistency among multiple dates. Thus, if there are only a few dates from a site or project, we cannot place much confidence in them (Fitzpatrick 2006; Spriggs 1989; Taché and Hart 2013). Comparison of multiple dates should proceed in the following stages: (1) among radiocarbon measurements from one excavation with direct or close stratigraphic relations among them; (2) among those from one site or one project that reflect consistent excavation procedures, stratigraphic interpretations, and ceramic phase assignments; and (3) among those from broad regions loosely connected through ceramic cross-dating.

Given the nature of archaeological deposits discussed above, we used the following general guidelines in this process:

(1) When multiple radiocarbon dates from the same context resulting from a single depositional event exhibit significant discrepancies, it is more likely that the youngest one is the closest to the true depositional date. In those cases, older dates possibly resulted from redeposited old materials.

(2) When radiocarbon dates from sequential ceramic phases or stratigraphic layers show a substantial overlap or reversal, it is more likely that those from the younger phases or upper layers are problematic dates resulting from the redeposition of old materials.

These general guidelines do not deny the possibility that the mixing of younger materials and chronometric problems resulted in more complex patterns. Thus, in our study we applied these criteria flexibly by examining specific archaeological contexts of individual cases. The evaluation process should not be a mechanistic application of fixed criteria.

*Bayesian Analysis*

The Bayesian analysis of radiocarbon dates incorporates prior information, usually on stratigraphic relations and ceramic phases, to produce a refined calibrated date for each radiocarbon measurement, which is called a posterior probability distribution. It can also provide estimates on the starting and ending dates of a given temporal phase. The analysis, however, does not rectify errors resulting from external factors, such as sample contamination, the lack of stratigraphic integrity, and the old wood effect. Problematic dates should be excluded from a model, hence the importance of identifying such dates. Researchers need to build a model based on various assumptions about the radiocarbon dates that they analyze, including phases (the time spans to which multiple samples belong to), sequences (the temporal order of radiocarbon samples or phases), and contemporaneity (one-time events/deposits to which multiple samples belong). Thus, Bayesian analysis is not a mechanical process. The validity of its results depends largely on the soundness of our archaeological interpretations, as well as appropriate choices of other prior information and of reliable radiocarbon measurements (Bayliss 2009). This also means that Bayesian analysis can serve as a heuristic tool to test both the adequacy of our assumptions on archaeological contexts and the integrity of radiocarbon measurements. Our main purpose for using Bayesian analysis was not to gain unexpected results that would be substantially different from our intuitive interpretations of radiocarbon dates, but to make our chronological assessment more robust by integrating different lines of evidence.

The application of Bayesian statistics to radiocarbon dates has been developed mainly in Britain (Bayliss 2009; Bronk Ramsey 2009; Buck and Millard 2004; Buck et al. 1991, 1996; Buck, Litton, and Smith 1994; Christen 1994), but there has been a recent increase in the use of Bayesian analysis in Mesoamerican archaeology (Bachand 2008; Beramendi-Orosco et al. 2009; Carleton et al. 2011; Culleton et al. 2012; Inomata et al. 2013; Kennett et al. 2011, 2013; Munson 2012). The application of Bayesian statistics to radiocarbon dates has been facilitated by the development of computer programs, including BCal (Buck et al. 1999) and DateLab (Jones and Nicholls 1999). For our analysis we used the OxCal 4.2.2 program with the IntCal09 calibration curve (Bronk 2013; Reimer et al. 2009). In the result outputs of OxCal, the premodeled distributions of calibrated date probabilities are indicated by light shading, whereas the modeled distributions of calibrated date probabilities (posterior probability distributions after the application of Bayesian statistics) are shown by solid fill. Bars below probability distributions indicate 95.4 percent probability ranges after the application of Bayesian statistics. A question mark at the end of a sample description identifies a problematic date that was excluded from the model (see Supplemental Text 4 for specific OxCal codes).

*Specific Approach in Our Study.* The qualities of radiocarbon dates and of associated archaeological information examined in this study are substantially different from one project to another. The inclusion of these different data in the same Bayesian model may skew the results. Thus, in most cases, we conducted Bayesian analyses separately for individual projects. The results of these Bayesian analyses were then compared across different projects and regions. For each case, we used Bayesian analysis mainly for two purposes: (1) to aid in the identification of problematic dates; and (2) to refine the remaining valid dates. Probability density plots generated in OxCal facilitate both processes. It is difficult enough to understand the relations between normal probability distributions of multiple uncalibrated radiocarbon dates. When dates are calibrated, they exhibit complex patterns of probability densities that do not conform to normal distributions. Visual representation is the most effective way to aid an intuitive understanding of their characteristics.

For the identification of problematic dates, OxCal indicates statistical outliers (dates that are probabilistically distant from others) primarily through agreement indices, that is, measures of the agreement between a premodeled calibrated date and its modeled posterior probability distribution. Bronk Ramsey (2013) recommends that agreement indices should usually be larger than 60 percent for a date to be considered valid. This means that a large part of the posterior density distribution of a modeled date should fall within the 2-sigma range of its premodeled calibrated date. However, this does not automatically mean that any dates with agreement indices lower than 60 percent are invalid. The exclusion of dates with agreement indices higher than 60 percent may results in better agreement indices for those dates that had poor indices in the previous model. Typically, we need to run Bayesian analysis multiple times with different sets of dates and other priors before reaching a conclusion on the most logical model. As discussed above, the evaluation of archaeological contexts is critical in this process. As Buck, Kenworthy, et al. (1994) put it, Bayesian statistics allows us to conduct “what if” analyses: if we use this information, what is the conclusion? The central utility of Bayesian analysis for archaeologists lies in its heuristic nature. By running multiple models with different priors, we can evaluate our choices of priors and their effects; this process makes our analysis more robust (Bayliss and Bronk  Ramsey 2004; Buck 2004).

In our discussion of the results of Bayesian analyses, we focused primarily on visual plots of probability densities, rather than on precise mean or median dates. This is partly because we did not wish to give the impression that those results are products of precise instrumental measurements and mathematics alone. We reiterate that the results of Bayesian analysis are substantially dependent on the interpretation of archaeological information—a process involving subjective judgments.

*Considerations on Potential Problems of Bayesian Analysis.* In evaluating the results of our analysis, we need to consider the potential problems of Bayesian statistics. One focus of debate concerning Bayesian analysis of radiocarbon dates and Bayesian statistics in general is the use of "uninformative priors" (Efron 2013). In contrast to "genuine" or "informative" priors that derive from observed data—such as stratigraphic relations— "vague" or "uninformative" priors refer to assumptions that are not based on observed data. There can be numerous uninformative priors that may potentially be applied to specific Bayesian models, but these uninformative priors are not based on concrete empirical data that would directly support one prior over another.

A more specific issue with direct relevance to the present study concerns phase boundaries, which are expressed by the Boundary function in OxCal. When radiocarbon measurements are made on materials from a given time period (phase), the span of observed measurements tends to become larger—i.e., the earliest date becomes earlier and the latest one later—as a larger number of measurements are made. This is simply because of the probabilistic nature of measurement errors: if more measurements are taken, there is a higher chance that measurements with larger errors will occur. Then, if we assume a simple uniform distribution in which the true dates of materials are totally independent, or unrelated to each other, and equally likely to occur at any point over an infinite time span, we tend to estimate a longer time span for a phase when we have more date measurements (Bayliss and Bronk 2004:37; Bronk 2001). This is clearly not acceptable. The same tendency occurs with ordered (sequential) dates (Nicholls and Jones 2001). If Bayesian analysis of sequential dates employs the assumption of their uniform distribution over an infinite time span as an uninformative prior (meaning that boundaries are not set in an OxCal model), the resulting posterior probabilities of individual dates may show artificially (unjustifiably) enhanced precision and they may deviate from their true ages (Steier and Rom 2000).

The application of boundaries to a phase is thus necessary in most cases. In such a model, the assumption applied as an informative prior is that the true date of each material is equally likely to occur anywhere within the limited time span defined by the given boundaries—which have unknown true dates—instead of the infinite time span of the previous case. The application of boundaries counteracts the tendency toward the expanding spread of measured dates correlated to the number of measurements (Buck 2004; Buck et al. 1992; Bronk Ramsey 1995, 2001:357). The argument by Steier and Rom (2000:197) that this use of boundaries and associated priors is no more valid than the use of an infinite time span is hardly tenable when we consider the foregoing reasoning (Bronk Ramsey 2000).

For certain sets of measured dates, Bayesian analysis may indicate shorter phase spans than most archaeologists would intuitively predict (see examples in Bayliss 2009; Bayliss et al. 2007). This tendency may be more notable when we are dealing with substantially overlapping measured dates that belong to a single phase. How much can we trust such results of Bayesian analysis? Our approach to this issue is rather conservative. We recognize a sound logic in the use of boundaries and associated uninformative priors in common Bayesian analysis. However, we do not place much confidence on Bayesian estimates of specific boundary dates for a single-phase set of dates. This is particularly true when we have largely overlapping dates—that is, dates with large error ranges in relation to the time span that they represent. We need to be cautious when the results of Bayesian analysis are significantly different from our intuitive understandings.

Under ideal conditions, Bayesian analysis may produce valid date estimates with very high precision out of low-precision data, as indicated by some simulations (see Bayliss 2009; Bayliss et al. 2007). This requires the following conditions: (1) the assumption of uniform distribution and other uninformed priors are appropriate; (2) the accuracies of individual measurements are high in relation to their precisions (or, at least, their deviations from the true dates are not skewed and conform to the expected probability distribution); and (3) individual measurements are not significantly affected by contamination, old wood problems, stratigraphic mixing, or reservoir effects. In reality, we usually cannot securely assume these conditions. When we have well-separated measured dates—which generally results from higher-precision measurements—our confidence level for the results of Bayesian analysis can be higher. Even without the use of boundary definitions, simulations conducted by Steier and Rom (2000) show adequate results of Bayesian analysis for well-separated dates.

Better priors for Bayesian estimates ultimately have to come in the form of observed data. In many archaeological situations, we have multiple phases defined by empirical information, including stratigraphy and ceramic phases. Whereas we remain cautious of Bayesian boundary estimates for single-phase data sets, we generally place significantly more confidence in estimates for a boundary between two phases. In the latter case, the boundary is strongly constrained by observed data, that is, by measured dates from the preceding and subsequent phases. Such a Bayesian model is based substantially on observed data, and the effects of uninformative priors become relatively weak. Under these conditions, Bayesian estimates generally conform well to our intuitive predictions. Thus, it is important for archaeologists to have some sense of the relative weight of uninformative priors in their models (see Berger 1994, 2006; Steier et al. 2001; Weninger et al. 2010 for mathematically based discussion of robust Bayesian analysis in relation to effects of uninformative priors).

In our data set, substantially overlapping dates for Providencia and Verbena-Arenal from the Museum of Tobacco and Salt excavation, for example, are not further constrained by dates from the preceding Las Charcas phase or those from the subsequent Santa Clara or Aurora phase (Figure 8). Thus, we do not place much confidence in the Bayesian estimates for the start date of Providencia and the end date of Arenal derived from this specific data set. However, the date for the transition from Providencia to Verbena is a different matter. It is more strongly defined by "genuine" or "informative" priors, that is, the dates from both phases constrain it from each side. Such a transition date suggested by Bayesian statistics should not be substantially different from intuitive predictions by most archaeologists. In the set of more recently obtained dates from Naranjo, Santa Isabel, and Kaminaljuyú—on which our chronology relies more strongly—each of the transition dates between Providencia, Verbena, Arenal, and Santa Clara is constrained by dates from the preceding and subsequent phases (Figure 10). In addition, because of their higher precision, these dates from different phases are relatively well separated. In this case, the posterior density distributions produced by Bayesian statistics are not much different from the premodeled distributions. In such a case, the resulting chronologies should not differ significantly, regardless of whether we use Bayesian statistics. All in all, substantially refined Bayesian-modeled dates from older projects accord well with those from new projects, on which the effects of Bayesian statistics are smaller. This supports the validity of our chronology and of Bayesian analysis.

*Problematic Calibration Curve Zone between 800 and 200 B.C.* Another issue we need to consider is the problematic zone in the radiocarbon calibration curve encompassing a plateau between 800 and 400 B.C. and a large upturn around 300 B.C. In this zone, even AMS dates with fairly high precisions exhibit large ranges of uncertainty when calibrated: from 800 to 400 B.C., or from 400 to 200 B.C. (Supplemental Figure 2). Thus, it is difficult to determine precise dates in this period even with the help of Bayesian analysis. Nonetheless, radiocarbon dates from the Middle Preclassic period (before 400 B.C.) and those from the Late Preclassic period (after 400 B.C.) generally show a clear separation (Supplemental Figure 2). For the purpose of our study, radiocarbon dates from these periods provide a sufficient basis with which to test our revised chronology against the Shook-Hatch chronology, particularly the question of whether the Providencia phase belongs to the Middle Preclassic or Late Preclassic period.

It is more challenging to determine the precise date of the transition from Las Charcas to Providencia. The shape of the calibration curve can give the illusion of a substantial gap between a set of pre-400 B.C. dates and a set of post-400 B.C. ones. In other words, most samples with true dates between 750 and 400 B.C. result in largely overlapping calibrated radiocarbon date ranges of roughly 800 to 400 B.C., whereas those with true dates between 400 and 200 B.C. show calibrated ranges of roughly 400 to 200 B.C. (Supplemental Figure 2). We should keep in mind that a sequence of samples with regular intervals from 800 to 200 B.C. can result in two internally undifferentiated sets of radiocarbon dates. In the Las Charcas date sets from Urías and Naranjo, most dates fall in the 800–400 B.C. range, but there are two (Beta-141170 from Urías and Beta-217153 from Naranjo) that correspond to the 400–200 B.C. range. In these cases—particularly for the Urías set, which has dates ordered by stratigraphic sequence—it is reasonable to think that the true ages of dates in the 400–200 B.C. range are close to the rest of the Las Charcas dates, that is, close to 400 B.C. Under these specific conditions, the uninformative prior of uniform distribution appears appropriate, and Bayesian analysis provides the expected results: modeled median dates of 371 B.C. for Beta-141170 and 376 B.C. for Beta-217153. These results lead us to suggest a tentative Las Charcas-Providencia transition date of 350 B.C. Readers who suspect that Bayesian analysis artificially shifts the Providencia phase forward in time should consider this: if we were to use the premodeled (not processed by Bayesian analysis) dates for these samples, they would suggest an even later Las Charcas-Providencia transition date of 300 or 200 B.C. This would be even more drastically different from the Shook-Hatch chronology.

In regard to the beginning of the Las Charcas phase, we need to be cautious about Bayesian results derived from the largely overlapping dates of the 800–400 B.C. range, for the reasons discussed above. For the data from Naranjo, the Bayesian model suggests a starting date for Las Charcas of 897–596 B.C. at the 95.4 percent probability level and 820–665 B.C. at the 68.2 percent level. We do not put much confidence in this estimate, and choose a fairly conservative date of 800 B.C. for the beginning of the main occupation at Naranjo. The premodeled 2-sigma calibrated dates from the Las Charcas phase of Naranjo fall predominantly after 800 B.C., and it is highly unlikely that their true dates are before 800 B.C. Although we recognize the possibility of earlier settlements not represented by these samples, it is reasonable to think that the main occupation of Naranjo did not start before 800 B.C. The beginning date of the Las Charcas occupation at Urías is more reliable. It is constrained by Beta-154187, which appears to predate the Las Charcas occupation.

## REFERENCES CITED


Bachand, Bruce R.

2008 Bayesian Refinement of a Stratified Sequence of Radiometric Dates from Punta De Chimino, Guatemala. *Radiocarbon* 50(1):19–51.

Bayliss, Alex

2009 Rolling Out Revolution: Using Radiocarbon Dating in Archaeology. *Radiocarbon* 51:123–147.

Bayliss, Alex, and Christopher Bronk Ramsey

2004 Pragmatic Bayesians: A Decade of Integrating Radiocarbon Dates into Chronological Models. In *Tools for Constructing Chronologies: Crossing Disciplinary Boundaries,* edited by Caitlin E. Buck and Andrew R. Millard, pp. 25–42. Springer, London.

Bayliss, Alex, Christopher Bronk Ramsey, Johannes van der Plicht, and Alasdair Whittle

2007 Bradshaw and Bayes: Towards a Timetable for the Neolithic. *Cambridge Archaeological Journal* 17:1–28.

Beramendi-Orosco, Laura, Galia Gonzalez-Hernandez, Jaime Urrutia-Fucugauchi, Linda Manzanilla, A. Soler-Arechalde, Avto Goguitchaishvili, and Nick Jarboe

2009 High-Resolution Chronology for the Mesoamerican Urban Center of Teotihuacan Derived from Bayesian Statistics of Radiocarbon and Archaeological Data. *Quaternary Research* 71(2):99–107.

Berger, James O.

1994 An Overview of Robust Bayesian Analysis. *Test* 3:5–124.

2006 The Case for Objective Bayesian Analysis. *Bayesian Analysis* 1:385–402.

Blockley, S. P. E., and R. Pinhasi

2011 A Revised Chronology for the Adoption of Agriculture in the Southern Levant and the Role of Lateglacial Climatic Change. *Quaternary Science Reviews* 30:98–108.

Bronk Ramsey, Christopher

1995 Radiocarbon Calibration and Analysis of Stratigraphy: The OxCal Program. *Radiocarbon* 37:425–430.

2000 Comment on "The Use of Bayesian Statistics for $^{14}$C Dates of Chronologically Ordered Samples: A Critical Analysis." *Radiocarbon* 42:199–202.

2001 Development of the Radiocarbon Calibration Program. *Radiocarbon* 43:355–363.

2009 Bayesian Analysis of Radiocarbon Dates. *Radiocarbon* 51:337–360.

2013 OxCal 4.2. Electronic resource, http://c14.arch.ox.ac.uk/embed.php?File=oxcal.html, accessed February 25, 2014.

Buck, Caitlin E.

2004 Bayesian Chronological Data Interpretation: Where Now? In *Tools for Constructing Chronologies: Crossing Disciplinary Boundaries*, edited by Caitlin E. Buck and Andrew R. Millard, pp. 25–42. Springer, London.

Buck, Caitlin E., William G. Cavanagh, and Clifford D. Litton

1996 Bayesian Approach to Interpreting Archaeological Data. Wiley, Chichester, England.

Buck, Caitlin E., J. Andrés Christen, and Gary N. James

1999 An On-Line Bayesian Radiocarbon Calibration Tool. *Internet Archaeology* 7. Electronic document. http://intarch.ac.uk/journal/issue7/buck_toc.html, accessed February 25, 2014.

Buck, Caitlin E., James B. Kenworthy, Clifford D. Litton, and Adrian F. M. Smith

1991 Combining Archaeological and Radiocarbon Information: A Bayesian Approach to Calibration. *Antiquity* 65(249):808–821.

1994 Reply to Reece. *Antiquity* 68:850.

Buck, Caitlin E., Clifford D. Litton, and Adrian F. M. Smith

1992 Calibration of Radiocarbon Dates Pertaining to Related Archaeological Events. *Journal of Archaeological Science* 19:497–512.

1994 Making the Most of Radiocarbon Dating: Some Statistical Considerations. *Antiquity* 68(259):252–263.

Buck, Caitlin E., and Andrew Millard

2004 *Tools for Constructing Chronologies: Crossing Disciplinary Boundaries.* Springer, London.

Carleton, Chris, Gyles Iannone, and James Conolly

2011 Dating Minanha Using a Bayesian Chronological Framework. In *Archaeological Investigations in the North Vaca Plateau, Belize: Progress Report of the Twelfth (2010) Field Season,* edited by Gyles Iannone, Jaime Awe, Maxime Lamoureux St-Hilaire and Matthew Longstaffe, pp. 109–131. Social Archaeology Research Program, Trent University, Peterborough.

Christen, J. Andrés

1994 Summarizing a Set of Radiocarbon Determinations: A Robust Approach. *Applied Statistics* 43:489–503.

Collett, David, and Peter Robertshaw

1983 Problems in the Interpretation of Radiocarbon Dates: The Pastoral Neolithic of East Africa. *African Archaeological Review* 1:57–74.

Culleton, Brendan J.

2006 Implications of a Freshwater Radiocarbon Reservoir Correction for the Timing of Late Holocene Settlement of the Elk Hills, Kern County, California. *Journal of Archaeological Science* 33:1331–1339.

Culleton, Brendan J., Keith M. Prufer, and Douglas J. Kennett

2012 A Bayesian AMS C14 Chronology of the Classic Maya Center of Uxbenká, Belize. *Journal of Archaeological Science* 39(5):1572–1586.

Efron, Bradley

2013 Bayes' Theorem in the 21st Century. *Science* 340:1177–1178.

Fitzpatrick, Scott M.

2006 A Critical Approach to 14C Dating in the Caribbean: Using Chronometric Hygiene to Evaluate Chronological Control and Prehistoric Settlement. *Latin American Antiquity* 17(4):389–418.

Hunt, Terry L., and Carl P. Lipo

2006 Late Colonization of Easter Island. *Science* 311:1603–1606.

Inomata, Takeshi, Daniela Triadan, Kazuo Aoyama, Victor Castillo, and Hitoshi Yonenobu

2013 Early Ceremonial Constructions at Ceibal, Guatemala, and the Origins of Lowland Maya Civilization. *Science* 340:467–471.

Jones, Martin, and Geoff Nicholls

1999 New Radiocarbon Calibration Software. *Radiocarbon* 44:663–674.

Keaveney, Evelyn M., and Paula J. Reimer

2012 Understanding the Variability in Freshwater Radiocarbon Reservoir Offsets: A Cautionary Tale. *Journal of Archaeological Science* 39:1306–1316.

Kennett, Douglas J., Brendan J. Culleton, Barbara Voorhies, and John Southon

2011 Bayesian Analysis of High-Precision AMS 14C Dates from a Prehistoric Mexican Shellmound. *Radiocarbon* 53:245–259.

Kennett, Douglas J., Irka Hajdas, Brendan J. Culleton, Soumaya Belmecheri, Simon Martin, Hector Neff, Jaime Awe, Heather V. Graham, Katherine H. Freeman, Lee Newsom, David L. Lentz, Flavio S. Anselmetti, Mark Robinson, Norbert Marwan, John Southon, David A. Hodell, and Gerald H. Haug

2013 Correlating the Ancient Maya and Modern European Calendars with High-Precision AMS 14C Dating. *Nature Scientific Reports* 3. Electronic document. http://www.nature.com/srep/2013/130411/srep01597/full/srep01597.html, accessed February 22, 2014.

Lanting, J. N., and J. van der Plicht

1994 14C AMS: Pros and Cons for Archaeology. *Palaeohistoria* 35/36:1–12.

Munson, Jessica

2012 Building on the Past: Temple Histories and Communities of Practice at Caobal, Petén, Guatemala. Unpublished Ph.D. dissertation, University of Arizona, Tucson.

Nicholls, Geoff, and Martin Jones

2001 Radiocarbon Dating with Temporal Order Constraints. *Applied Statistics* 50:503–521.

Nolan, Kevin C.

2012 Temporal Hygiene: Problems in Cultural Chronology of the Late Prehistoric Period of the Middle Ohio River Valley. *Southeastern Archaeology* 31(2):185–206.

Pendergast, David M.

2000 The Problems Raised by Small Charcoal Samples for Radiocarbon Analysis. *Journal of Field Archaeology* 27(2):237–239.

Pettitt, P. B., W. Davies, C. S. Gamble, and M. B. Richards

2003 Palaeolithic Radiocarbon Chronology: Quantifying our Confidence Beyond Two Half-Lives. *Journal of Archaeological Science* 30(12):1685–1693.

Reimer, P. J., M. G. L. Baillie, E. Bard, A. Bayliss, J. W. Beck, P. G. Blackwell, C. B. Ramsey, C. E. Buck, G. S. Burr, and R. L. Edwards

2009 IntCal09 and Marine09 Radiocarbon Age Calibration Curves, 0–50,000 Years Cal BP. *Radiocarbon* 51(4):1111–1150.

Spriggs, Matthew

1989 The Dating of the Island Southeast Asian Neolithic: An Attempt at Chronometric Hygiene and Linguistic Correlation. *Antiquity* 63(240):587.

Steier, Peter, and Werner Rom

2000 The Use of Bayesian Statistics for 14C Dates of Chronologically Ordered Samples: A Critical Analysis. *Radiocarbon* 42:183–198.

Steier, Peter, Werner Rom, and Stephan Puchegger

2001 New Methods and Critical Aspects in Bayesian Mathematics for 14C Calibration. *Radiocarbon* 43:373–380.

Taché, Karine, and John P. Hart

2013 Chronometric Hygiene of Radiocarbon Databases for Early Durable Cooking Vessel Technologies in Northeastern North America. *American Antiquity* 78(2):359–372.

Telford, Richard J., Einar Heegaard, and Harry John Betteley Birks

2004 The Intercept Is a Poor Estimate of a Calibrated Radiocarbon Age. *Holocene* 14:296–298.

Waterbolk, H. T.

1971 Working with Radiocarbon Dates. *Proceedings of the Prehistoric Society* 37:15–33.

Waters, Michael R., and Thomas W. Stafford

2007 Redefining the Age of Clovis: Implications for the Peopling of the Americas. *Science* 315:1122–1126.

Weninger, Franz, Peter Steier, Walter Kutschera, and Eva Maria Wild

2010 Robust Bayesian Analysis, an Attempt to Improve Bayesian Sequencing. *Radiocarbon* 52:962–983.

Wilmshurst, Janet M., Terry L. Hunt, Carl P. Lipo, and Atholl J. Anderson

2011 High-Precision Radiocarbon Dating shows Recent and Rapid Initial Human Colonization of East Polynesia. *Proceedings of the National Academy of Sciences* 108:1815–1820.

**Supplemental Text 2. Evaluation of the Stratigraphy of the Museum of Tobacco and Salt (MTS) Excavations at Kaminaljuyú**

What MTS researchers called Period II is represented by an early version of Mound B-I-1, which they called “Edificio Quemado.” In the southeastern part of the building, the excavators found traces of burning. After this burning event, the Edificio Quemado was buried by Floor 4 and by the next version of Mound B-I-1, which they called the “Gran Basamento” (Supplemental Figure 3). Around the Edificio Quemado, excavators uncovered a series of burials and caches. Burials 2 and 3 were placed in the construction layer of the Gran Basamento. The stratigraphic position of Burial 5 is less clear. Their interpretation was that the caches were placed at the time of construction of the Gran Basamento. Ceramics found in these burials and caches largely correspond to the Providencia complex, characterized by labial/medial flanges, scalloped ridges, Kaminaljuyú Black-Brown with coarse incisions, and Xuc ware. Burials 2 and 5 contained a small number of bowls with nubbin feet, which are characteristic of the Verbena phase, but other clear Verbena markers, such as Kaminaljuyú Black-Brown with fine incisions, are absent. These data indicate that the Edificio Quemado was in use during the Providencia phase and that the next version was constructed at the transition to the Verbena phase.

MTS researchers interpreted the samples taken from the burned area—Gak-17124, Gak-171129, and NUTA-2110—as construction materials of the Edificio Quemado. Gak-17925 was taken from one of the caches. Following their interpretation, our Bayesian model assumes that Gak-17124, Gak-171129, and NUTA-2110 represent the use period of the building and Gak-17925 the end of its use. However, it may also be possible that Gak-17124, Gak-171129, and NUTA-2110 include fuel placed at the time of burning. Gak-17925 is older than Gak-17129 and NUTA-2110, and may be somewhat old wood. Gak-17928, taken from D-III-1, is a clear outlier.

During the following Period III, Floors 3 and 2 were constructed. Excavators found numerous caches, with a total of 100 vessels placed on Floor 4 at the time of construction of Floor 3. These assemblages consist of typical Verbena types, such as Kaminaljuyú Black-Brown with fine incisions and wavy-line Usulután. They also include a small number of Arenante Coarse Incised vessels, which Popenoe de Hatch (1997) lists as a diagnostic type of the Arenal phase. However, other markers of the Arenal phase, such as larger supports, are absent. We interpret these deposits to have been made near the end of the Verbena phase or at the transition to the Arenal phase. At the time of the construction of Floor 2, caches with a total of eight vessels were deposited. These vessels are of general Verbena-Arenal types, but we assume that this construction occurred during the Arenal phase.

MTS researchers obtained eight radiocarbon dates from charcoal collected from the caches found on Floor 4. Four of these dates are clear outliers. Among the remaining four measurements, Gak-17127 and NUTA-2084 are older than NUTA-2109 and NUTA-2056, although they show a substantial overlap. In our Bayesian model, we assumed that the former two were somewhat old wood, and combined the latter two. Gak-17926 was collected from one of the caches found on Floor 3. It is older than the dates from the caches found on Floor 4 and was excluded as an outlier. Gak-17927, taken from a Period-III layer of D-III-1, accords well with the dates from the caches found on Floor 4.

## Supplemental Text 3. Evaluation of the Stratigraphic Position of Monument 1 at El Portón, Salamá Valley

According to excellent stratigraphic descriptions and drawings by Sharer and Sedat (1987), Monument 1 was placed in a small enclosure opening to the west, Structure J7-4B-5, which was found in front of (to the west of) a platform building, J7-4A (Supplemental Figure 5). Structures J7-4A and J7-4B were built directly on the Max-phase fill of the basal platform, and Structure J7-4A went through at least three renovations during the Tol phase, which were named J7-4A-3, J7-4A-2, and J7-4A-1, from the oldest to the newest. The area between Structure J7-4A and J7-4B was not excavated, and thus the precise stratigraphic relation between the two buildings is not clear. Still, it appears more likely that J7-4B-5 was built after J7-4A-1, whose front portion sat directly on the Max-phase floor and then was abutted by a sequence of floors and fills associated with J7-4B. The fill of a floor resurfacing (U10B) of J7-4B-5, which was presumably made after Monument 1, contained Tol ceramics, whereas the fill of the next version of the building, J7-4B-4, contained Uc pottery. Sharer's interpretation was that Cache 25 and the skull deposit (Burial 2)—placed on the Max-phase floor and covered by J7-4B-5—were dedicatory offerings deposited at the time when Structure J7-4B-5 was constructed and Monument 1 was erected. Ceramics found in these offerings were classified as belonging to the Tol phase, but they are not diagnostic enough for more precise dating. This construction sequence suggests that Structure J7-4B-5 and Monument 1 date to the late or final part of the Tol phase.

P-2134 and P-2135—taken from a pit (F3A) dug into the Max-phase floor and covered by Structure J7-4A-3—define the earliest possible date for the construction of this building, with the highest probability around 270 B.C. P-2132, which Sharer used to date Monument 1, was taken from a dedicatory cache (Cache 25) found 9 m to the east of Monument 1. With the assumption that P-2132 stratigraphically postdates P-2134 and P-2135, the Bayesian model places the most likely age for P-2132 around 230 B.C. P-2133, taken from a hearth cut into Structure J7-4B-4, shows a date of around A.D. 30. In other words, the median date of P-2132 is considerably closer to those of P-2134 and P-2135 than to that of P-2133.

We suspect that P-2133 might be somewhat old wood. Considering the ceramic data, we suggest that the most likely date for the erection of Monument 1 is around 100 B.C. A date of 400 B.C. is highly unlikely.

## Supplemental Text 4. OxCal Code

**Kaminaljuyú: Carnegie Dates**

```
Plot()
 {
  Sequence("Kaminaljuyu")
  {
   Phase("Arevalo")
   {
    R_Date("Y-401 C-III-10 2nd Str.", 2240, 60)
    {
     Outlier();
    };
    R_Date("Y-402 C-III-10 sandy layer over sterile", 2070, 50)
    {
     Outlier();
    };
   };
   Boundary("Start Las Charcas");
   Phase("Las Charcas")
   {
    R_Date("Y-384 Finca Las Charcas, Late Las Charcas", 2340, 50);
    R_Date("M-1257 Finca Las Charcas", 2280, 130);
   };
   Boundary("Las Charcas-Majadas");
   Phase("Majadas")
   {
    R_Date("Y-390 C-III-6 Intrusive pit", 2335, 50);
    R_Date("C-886 C-III-6 same as Y-390", 2970, 200)
    {
     Outlier();
    };
   };
   Boundary("Majadas-Providencia");
   Phase("Providencia")
   {
    R_Date("Y-370 D-III-10 older construction", 1850, 60)
    {
     Outlier();
    };
    R_Date("C-879 D-III-10 same as Y-370", 3130, 300)
    {
     Outlier();
    };
    R_Date("Y-374 Zacat, Sacatepequez, Pit R 3", 2120, 60);
   };
   Boundary("Providencia-Verbena");
```

```
   Phase("Verbena")
   {
    Sequence("Verbena")
    {
     R_Date("Y-382 E-III-3 Str. 3b, 3c, 3d, 4 fill", 1920, 60);
     R_Date("C-884 E-III-3 same as Y-382", 3142, 240)
     {
      Outlier();
     };
     R_Date("Y-391 E-III-3 Str. 5 fill", 2025, 60)
     {
      Outlier();
     };
     R_Date("C-887 E-III-3 same as Y-391", 2490, 300)
     {
      Outlier();
     };
     R_Date("Y-377 E-III-3 Tomb 1", 1940, 60);
    };
   };
   Boundary("Verbena-Arenal");
   Boundary("Arenal-Santa Clara");
   R_Date("Y-406 D-III-1, midden sealed by terrace fill", 1800, 60);
   Boundary("Santa Clara-Aurora");
   Sequence("Aurora")
   {
    R_Date("Y-405 D-III-13 adobe str fill below Str. K", 1660, 60);
    R_Date("Y-378 D-III-13", 1785, 60);
    Phase("")
    {
     R_Date("Y-396 D-III-13 Post hole str. Floors 2 and 3", 1860, 60)
     {
      Outlier();
     };
     R_Date("Y-629 D-III-13 below burial above stone", 1560, 70);
    };
   };
   Boundary("End Aurora");
  };
 };
```

**Kaminaljuyú: Penn State Dates**

```
Plot()
 {
  Sequence("Penn State Kaminaljuyu")
  {
   Boundary("Start Providencia");
```

```
  Phase("Providencia")
  {
   R_Date("I-6250", 2355, 90);
   R_Date("I-6610", 2215, 90);
   R_Date("I-6384", 2205, 180);
   R_Date("I-6247", 1865, 150)
   {
    Outlier();
   };
  };
  Boundary("Providencia-Verbena");
  Phase("Verbena")
  {
   R_Date("I-6249", 2090, 90);
   R_Date("I-6305", 2060, 90);
  };
  Boundary("Verbena-Arenal");
  Phase("Arenal")
  {
   R_Date("I-6248", 1965, 90);
   R_Date("I-6332", 1830, 90);
  };
  Boundary("Arenal-Aurora");
  R_Date("I-6269", 1915, 90);
  Boundary("Aurora-Esperanza");
  R_Date("I-6308", 1750, 90);
  Boundary("Esperanza-Amatle");
  R_Date("I-6270", 1225, 90);
  Boundary("End Amatle");
 };
};
```

**Semetabaj Dates**

```
Plot()
 {
  Sequence("San Andres Semetabaj")
  {
  R_Date("GX-5859 Pit 2 plaza fill", 2660, 175)
  {
   Outlier();
  };
  Boundary("Providencia-Verbena/Arenal");
  Phase("Verbena-Arenal")
  {
   Sequence("platforms")
   {
    R_Date("GX-5856 Burned main post, lower platform", 1840, 120);
```

```
   R_Date("GX-5857 Burned main post, upper platform", 1865, 130);
   };
   R_Date("GX-5858 Pit 7 plaza fill", 1960, 135);
  };
  Boundary("Verbena/Arenal-Early Classic");
  R_Date("GX-5860 Pit 4, intrusive pit", 1485, 140);
  Boundary("End Early Classic");
 };
};
```

**Kaminaljuyú: Museum of Tobacco and Salt Dates**

```
Plot()
 {
 Sequence("Kaminaljuyu: MTS")
 {
  Boundary("Start Providencia");
  Phase("Providencia")
  {
   R_Date("GaK-17928 D-III-1 on Str. 5 floor", 2930, 90)
   {
    Outlier();
   };
   Sequence("Burned Str.")
   {
    Phase("Burned Str. use")
    {
     R_Date("GaK-17124 Burned Str.", 2330, 160);
     R_Date("GaK-17129 Burned Str.", 2210, 120);
     R_Date("NUTA-2110 Burned Str.", 2140, 130);
    };
    Boundary();
    R_Date("GaK-17925 Under Floor 4 Offering 62", 2270, 200);
   };
  };
  Boundary("Providencia-Verbena/Arenal");
  Phase("Verbena-Arenal")
  {
   R_Date("GaK-17128 On Floor 4 Offering 16", 3750, 300)
   {
    outlier();
   };
   R_Date("GaK-17125 On Floor 4 Offering 23", 3000, 110)
   {
    outlier();
   };
   R_Date("GaK-17126 On Floor 4 Offering 17", 2970, 90)
   {
```

```
   outlier();
  };
  R_Date("GaK-17123 On Floor 4 Offering 19", 2540, 90)
  {
   outlier();
  };
  R_Date("GaK-17127 On Floor 4 Offering 26", 2070, 130)
  {
   outlier();
  };
  R_Date("NUTA-2084 On Floor 4 Offering 57", 2060, 180)
  {
   outlier();
  };
  R_Combine("Floor 4 NUTA-2109xNUTA-2056")
  {
   R_Date("NUTA-2109 On Floor 4 Offering 24", 1950, 130);
   R_Date("NUTA-2056 On Floor 4 Offering 29", 1920, 160);
  };
  R_Date("GaK-17926 On Floor 3", 2200, 70)
  {
   Outlier();
  };
  R_Date("GaK-17927 D-III-1 on Str. 4 floor", 2060, 80);
 };
 Boundary("End Arenal");
};
};
```

**Urías Dates**

```
Plot()
 {
 Sequence("Urias")
 {
  Boundary("Start Urias sequence");
  R_Date("Beta-154187 Subop 8 Nivel 25", 2810, 40);
  Boundary("Start Agua");
  R_Date("Beta-114963 Subop 6 Nivel 24", 3260, 120)
  {
   Outlier();
  };
  Phase("Level 21")
  {
   R_Date("Beta-114962 Subop 2 Nivel 21 midden", 2460, 60);
   R_Date("Beta-141169 Subop 7 Nivel 21", 2370, 50);
  };
  R_Date("Beta-141168 Subop 8 Nivel 19 midden", 2570, 100);
```

```
  Phase("Level 18")
  {
   R_Date("Beta-114966 Subop 2 Nivel 18 midden", 2510, 60);
   R_Date("Beta-114961 Subop 3 Nivel 18", 2380, 60);
  };
  R_Date("Beta-114960 Subop 3 Nivel 17 stela", 2430, 60);
  R_Date("Beta-141170 Subop 7 Nivel 16 burial", 2250, 50);
  Boundary("End Agua");
 };
};
```

**Naranjo, Santa Isabel, Kaminaljuyú Park, Miraflores II Project, and Brigham Young-Del Valle Dates**

```
Plot()
 {
 Sequence("Naranjo-Kaminaljuyu")
 {
  Boundary("Start Las Charcas");
  Sequence("Naranjo-Santa Isabel")
  {
   Phase("Early Las Charcas")
   {
    //     R_Date("Beta-214073 N. Mon. 7", 4600, 40)
    //     {
    //      Outlier();
    //     };
    R_Date("Beta-214075 N. Mon. 3", 2550, 40);
    R_Date("Beta-215654 N. N. Sec.", 2550, 40);
    R_Date("Beta-215653 N. S Plat.", 2500, 40);
    R_Date("Beta-220576 N. Mound 1", 2430, 40);
   };
   R_Date("Beta-209872 N. N. Plat.", 2590, 60);
   Phase("Late Las Charchas")
   {
    R_Date("Beta-215655 N. Mon. 22", 2510, 40);
    R_Date("Beta-217153 N. SW S.", 2270, 40);
    //     R_Date("Beta-217152 N. Hearth", 560, 50)
    //     {
    //      Outlier();
    //     };
    R_Date("Beta-307568 Sta Isabel", 2450, 30);
    R_Date("Beta-307569 Sta Isabel", 2410, 30);
   };
  };
  Boundary("Las Charcas-Providencia");
  Phase("Providencia")
  {
   R_Date("Beta-164710 Miraflores II", 2060, 60);
```

```
};
Boundary("Providencia-Verbena");
Phase("Verbena")
{
 R_Date("Beta-164706 Miraflores II", 2020, 40);
 R_Date("Beta-361803 Mound E-III-5", 1990, 30);
};
Boundary("Verbena-Arenal");
Phase("Arenal")
{
 R_Date("Beta-320689 KJ Palangana south wall initial deposit", 2120, 30)
 {
  Outlier();
 };
 R_Date("Beta-320688 KJ C-II-12 base Palangana dedicatory", 2050, 30)
 {
  Outlier();
 };
 R_Date("Beta-307567 KJ early deposit Acropolis", 1960, 30);
 R_Date("Beta-164707 Miraflores II", 1180, 60)
 {
  Outlier();
 };
};
R_Date("Beta-307565 KJ Acropolis End Arenal", 1930, 30);
Phase("Santa Clara")
{
 R_Date("Beta-164709 Miraflores II", 2140, 40)
 {
  Outlier();
 };
 R_Date("Beta-361800 Palangana West wall", 1790, 30);
 R_Date("Beta-361798 Palangana West wall", 1820, 30);
};
Boundary("Santa Clara-Aurora");
Phase("Aurora")
{
 R_Date("Beta-164708 Miraflores II", 2040, 40)
 {
  Outlier();
 };
 R_Date("Beta-361801 Palangana, East wall", 1660, 30);
};
Boundary("Aurora-Esperanza");
Phase("Esperanza")
{
 Sequence("BYU Acropolis")
 {
```

```
    R_Date("AA-55657 Earliest talud-tablero Str. E", 1520, 35);
    Phase()
    {
     R_Date("AA-57122 ", 1590, 80);
     R_Date("AA-57655 ", 1510, 30);
    };
    R_Date("AA-57656 Last talud-tablero", 1475, 30);
   };
   Sequence("Parque")
   {
    R_Date("Beta-320687 KJ Early Esperanza", 1670, 30);
    R_Date("Beta-320690 KJ Late Esperanza", 1470, 30);
   };
  };
  Boundary("Esperanza-Amatle");
  Phase("Amatle")
  {
   R_Date("Beta-361802 Mound C-II-13", 1860, 30)
   {
    outlier();
   };
   R_Date("Beta-307566 KJ Acropolis tunnel Late Classic", 1400, 30);
   R_Date("Beta-320691 KJ Late Classic", 1310, 30);
   R_Date("Beta-220578 Naranjo North S.", 1250, 60);
   R_Date("Beta-220577 Naranjo South Plat.", 1260, 60);
   R_Date("AA-13080 Str. F", 1180, 150);
   //    R_Date("Beta-220579 Naranjo South Plat.", 2190, 40)
   //    {
   //     Outlier();
   //    };
  };
  Boundary("Amatle-Pamplona");
  Phase("Pamplona")
  {
   R_Date("Beta-361799 Palangana, South wall", 1210, 30);
   R_Date("Beta-361804 Área ceremonial contemporánea", 1190, 30);
  };
  Boundary("End Pamplona");
 };
};
```

**Chalchuapa-Santa Leticia Dates**

```
Plot()
 {
  Sequence()
  {
   Boundary("Start Tok");
```

```
  R_Date("P-1551 C", 2790, 57);
  Boundary("Tok-Colos");
  Phase("Colos")
  {
   R_Date("P-1807 C", 2448, 60);
   R_Date("P-1806 C", 2385, 63);
  };
  Boundary("End Colos");
  Boundary("Start Chul");
  Phase("Chul")
  {
   R_Date("Q-3108 SL", 2320, 100);
   R_Date("Q-3105 SL", 2090, 85);
   R_Date("Q-3101 SL", 2035, 90);
   R_Date("Q-3106 SL", 1940, 90);
  };
  Boundary("Chul-Early Caynac");
  Phase("Early Caynac")
  {
   R_Date("P-1550 C", 2036, 44);
   R_Date("P-1805 C", 1965, 61);
   R_Date("Q-3104 SL", 1930, 80);
   R_Date("Q-3109 SL", 1930, 90);
   R_Date("Q-3102 SL", 1870, 65);
   R_Date("Q-3103 SL", 1775, 85)
   {
    outlier();
   };
  };
  Boundary("Early Caynac-Late Caynac");
  R_Date("P-1547 C", 1817, 38);
  Boundary("Late Caynac-Vec");
  R_Date("P-1803 C", 1717, 62);
  Boundary("End Vec");
 };
};
```

**Salamá Valley Dates**

```
Plot()
 {
  Sequence("Salama")
  {
   Boundary("Start Early Xox");
   R_Date("P-3208 Sakajut", 2880, 190);
   Boundary("End Early Xox");
   Boundary("Start Max");
   R_Date("P-2139 Mangales D6-2 U1", 2290, 50);
```

```
  Boundary("Max-Tol");
  Phase("Tol")
  {
   Sequence("El Porton J7-2")
   {
    R_Date("P-2137 El Porton F21", 2230, 60);
    R_Date("P-2136 El Porton F19", 2160, 60);
    R_Date("P-2138 El Porton C32", 2320, 50)
    {
     Outlier();
    };
   };
   Sequence("El Porton J7-4")
   {
    R_combine("El Porton J7-4A-3 F3A: P-2135xP-2134")
    {
     R_Date("P-2135 El Porton F3A", 2230, 60);
     R_Date("P-2134 El Porton F3A", 2300, 50);
    };
    R_Date("P-2132 El Porton C25", 2260, 60);
   };
   Sequence("Las Tunas C6-1")
   {
    R_Date("P-2220 Las Tunas F2B", 2180, 60);
    R_Date("P-2219 Las Tunas F3", 2140, 70);
   };
   R_Date("P-2221 Las Tunas C6-2 F5", 2020, 60);
   R_Date("P-2222 Las Tunas C6-2 U11", 2300, 50)
   {
    Outlier();
   };
  };
  Boundary("Tol-Uc");
  R_Date("P-2133 El Porton F8", 1960, 40);
  //    Date(Archmag776,N(15.5,13));
  Boundary("End Uc");
 };
};
```

**La Lagunita Dates**

```
Plot()
 {
  Sequence("La Lagunita")
  {
   R_Date("Gif-4556 EJ-16", 1900, 90)
   {
    Outlier();
```

```
   };
   Boundary("Start Lililla 1");
   R_Date("Gif-4231 Burial S-2", 1870, 100);
   Boundary("Lililla 1-Lililla 2");
   R_Date("Gif-4230 C-43 Floor IIa cache", 1640, 90);
   Boundary("Lililla 2-Lililla 3");
   Phase("Lililla 3")
   {
    Phase("C-44 Tomb")
    {
     Phase("Ceramic bowl")
     {
      R_Date("I-10014 C-44/183", 1840, 95)
      {
       Outlier();
      };
      R_Date("Gif-4228 C-44/183", 1630, 90);
     };
     R_Date("Gif-4229 C-44/B4-1", 1480, 90);
    };
    Phase("C-48 cave")
    {
     R_Date("Gif-4555 C2/18", 1650, 80);
     R_Date("Gif-4554 E4/10", 1640, 80);
     R_Date("Gif-4553 B8/25", 1610, 80);
     R_Date("UCLA-2138", 1530, 80);
     R_Date("I-10011", 1505, 100);
     R_Date("Gif-4227 108", 1350, 90)
     {
      Outlier();
     };
    };
   };
   Boundary("End Lililla 3");
  };
 };
```

**Izapa Dates**

```
Plot()
 {
  Sequence("Izapa")
  {
   Boundary("Start Duende");
   Phase("Duende")
   {
    Phase("30a-D4")
    {
```

```
  R_Date("I-1656 M30a, Exc. L, Level 14", 2580, 220);
  R_Date("I-1655 M30a, Exc. L, Level 10-11", 2310, 210);
 };
 R_Date("I-873 M30a, Exc. D, on floor", 2695, 100);
};
Boundary("Duende-Frontera");
Phase("Frontera")
{
 R_Date("I-1660 M30a, Exc. L, Str. F1a2, on burned plat.", 2600, 130);
 R_Date("I-4854 M59, Exc. A, Sec. 5 ash line", 2440, 130);
 R_Date("I-1218 M25, Exc. A, primary desposit on sterile", 2280, 150);
 R_Date("I-4855 M59, Exc. A, Sec. 5-6", 2280, 90);
};
Boundary("Frontera-Gap");
Boundary("Gap-Guillen");
R_Date("I-875 M30a, Exc. D, F. 1", 2100, 95);
Phase("Guillen")
{
 R_Date("I-876 M58, Exc. 1, on floor", 2695, 120)
 {
  Outlier();
 };
 R_Date("I-872 M61, Exc. B, Sec. N4, F. 2", 2205, 95);
 R_Date("I-877 M60, Exc. A, Level 12, on floor", 2100, 90);
 R_Date("I-1211 M60, Exc. A, hearth/posthole", 1855, 140);
};
Boundary("Guillen-Hato");
R_Date("I-871 M30a, B, inside partial vessel", 2100, 110)
{
 Outlier();
};
Boundary("Hato-Itstapa");
Sequence("Itstapa")
{
 Phase("Floor 3 fill")
 {
  R_Date("I-4548 M125a, Exc. A, below Floor 3", 1830, 95);
  R_Date("I-1654 M125a, Exc. A, F. 89-4", 1790, 150);
 };
 R_Date("I-1653 M125a, Exc. A, on floor 3", 1850, 200);
};
Boundary("Itstapa-Jaritas");
R_Date("I-1210 M125a, Exc. A, F. 51", 1565, 145);
Boundary("Jaritas-Kato");
R_Date("I-1217 M125a, Exc. A, F. 26", 2330, 220)
{
 Outlier();
};
```

```
  Boundary("Kato-Loros");
  R_Date("I-4545 M125b, Exc. A, F. 63", 1700, 125);
  Boundary("Loros-Peistal");
  Phase("Peistal")
  {
   R_Date("I-4547 M125c, Exc. B, F. 84, Tomb 4", 1180, 100);
   R_Date("I-4544 M125, Exc. B, F. 62", 1155, 100);
  };
  Boundary("Peistal-Remanso");
  R_Date("I-1214 M125a, Exc. A, F. 13", 2400, 235)
  {
   Outlier();
  };
  R_Date("I-4546 M130, Exc. B, F. 64, hearth", 1060, 100);
  Boundary("End Remanso");
 };
};
```

**San Bartolo Dates**

```
Plot()
{
 Sequence("San Bartolo")
 {
  Boundary("Start Sub-VI");
  R_Date("Beta-206576 Sub-VI in floor", 2260, 40);
  Boundary("Sub-VI to Sub-V");
  R_Date("Beta-206577 Sub-V in floor", 2200, 60);
  Boundary("Sub-V construction to destruction");
  R_Combine("Sub-V destruction 206624x206578x206575")
  {
   R_Date("Beta-206624 Sub-V destruction", 2260, 40);
   R_Date("Beta-206578 Sub-V destruction", 2180, 40);
   R_Date("Beta-206575 Sub-V destruction", 2150, 40);
  };
  Boundary("Sub-V destruction to Sub-IV");
  Boundary("Sub-II to Sub-I");
  R_Date("Beta-193509 Sub-I mural plaster wall", 2140, 40);
  Boundary("Sub-I construction to termination");
  R_Date("Beta-193510 Sub-I on floor burning", 2070, 40);
  Phase("Final construction")
  {
   R_Date("Beta-193512 Final construction", 2100, 40);
   R_Date("Beta-193513 Final construction", 2050, 40);
   R_Date("Beta-193511 Final construction", 2050, 50);
  };
  Boundary("End final construction");
 };
```

```
};
```

Supplemental Figure 1. Ceramic cross-dating from Shook's notebook.

Supplemental Figure 2. Radiocarbon calibration curve and an OxCal simulation showing how calibrated radiocarbon dates obtained from samples with true dates between 850 B.C. and 150 B.C., spaced at regular intervals of 100 years, might distribute (uncertainty of 30 years). Note that they give a false impression that two discrete groups of dates might exist in the 800–400 B.C. and 400–200 B.C. ranges.

Supplemental Figure 3. Stratigraphic sequence of the excavations by the Museum of Tobacco and Salt.

Supplemental Figure 4. The results of Bayesian analysis of radiocarbon dates obtained from Classic-period contexts from Naranjo, the Kaminaljuyú Park, the Miraflores II Project, and the Brigham Young University-Universidad del Valle excavations.

Supplemental Figure 5. Stratigraphic sequence related to Monument 1, El Portón, Salamá Valley.

Supplemental Figure 6. The results of Bayesian analysis of radiocarbon dates obtained from La Lagunita, Chixoy River Valley.

Supplemental Figure 7. The results of Bayesian analysis of radiocarbon dates obtained from Izapa.

Supplemental Figure 8. The results of Bayesian analysis of radiocarbon dates obtained from San Bartolo.

Supplemental Table 1. Radiocarbon dates from Kaminaljuyú and other regions.

Supplemental Table 2. Ceramic cross-dating of Kaminaljuyú and relevant regions with diagnostic types and modes.

| Years | Kaminaljuyú | Uaxactún |
|---|---|---|
| 500 | | |
| 400 | Esperanza | Tzakol 3 |
| 300 | | |
| 200 | Salcaja | Tzakol 2 |
| 100 | | Tzakol 1 |
| 1 A.D. / B.C. | Salcaja | (Holmul II) |
| 100 | | |
| 200 | Salcaja | Matzanel |
| 300 | | (Holmul I) |
| 400 | | |
| 500 | Santa Clara | |
| 600 | | |
| 700 | | |
| 800 | Arenal | |
| 900 | | |
| 1000 | | |
| 1100 | | |
| 1200 | Verbena | Chicanel |
| 1300 | | |
| 1400 | Providencia | |
| 1500 | | |
| 1600 | | |
| 1700 | Sacatepéquez | |
| 1800 | Mound C-III-6 | |
| 1900 | | |
| 2000 | | |
| 2100 | | Mamom |
| 2200 | | |
| 2300 | | |
| 2400 | | |
| 2500 | Las Charcas | |
| 2600 | | |
| 2700 | | |
| 2800 | | |
| 2900 | | |
| 3000 | | |

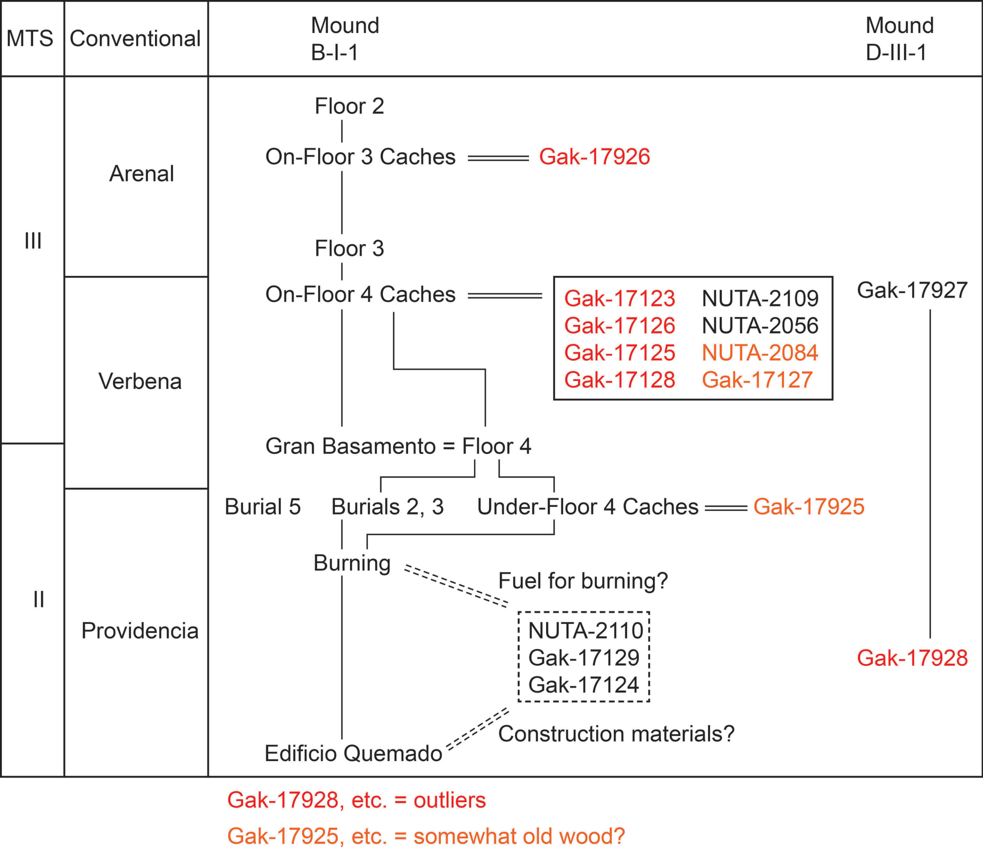
MTS
Conventional
Mound B-I-1
Mound D-III-1
III
II
Arenal
Verbena
Providencia
Floor 2
On-Floor 3 Caches
Gak-17926
Floor 3
On-Floor 4 Caches
Gak-17123
Gak-17126
Gak-17125
Gak-17128
NUTA-2109
NUTA-2056
NUTA-2084
Gak-17127
Gak-17927
Gran Basamento = Floor 4
Burial 5
Burials 2, 3
Under-Floor 4 Caches
Gak-17925
Burning
Fuel for burning?
NUTA-2110
Gak-17129
Gak-17124
Gak-17928
Construction materials?
Edificio Quemado
Gak-17928, etc. = outliers
Gak-17925, etc. = somewhat old wood?

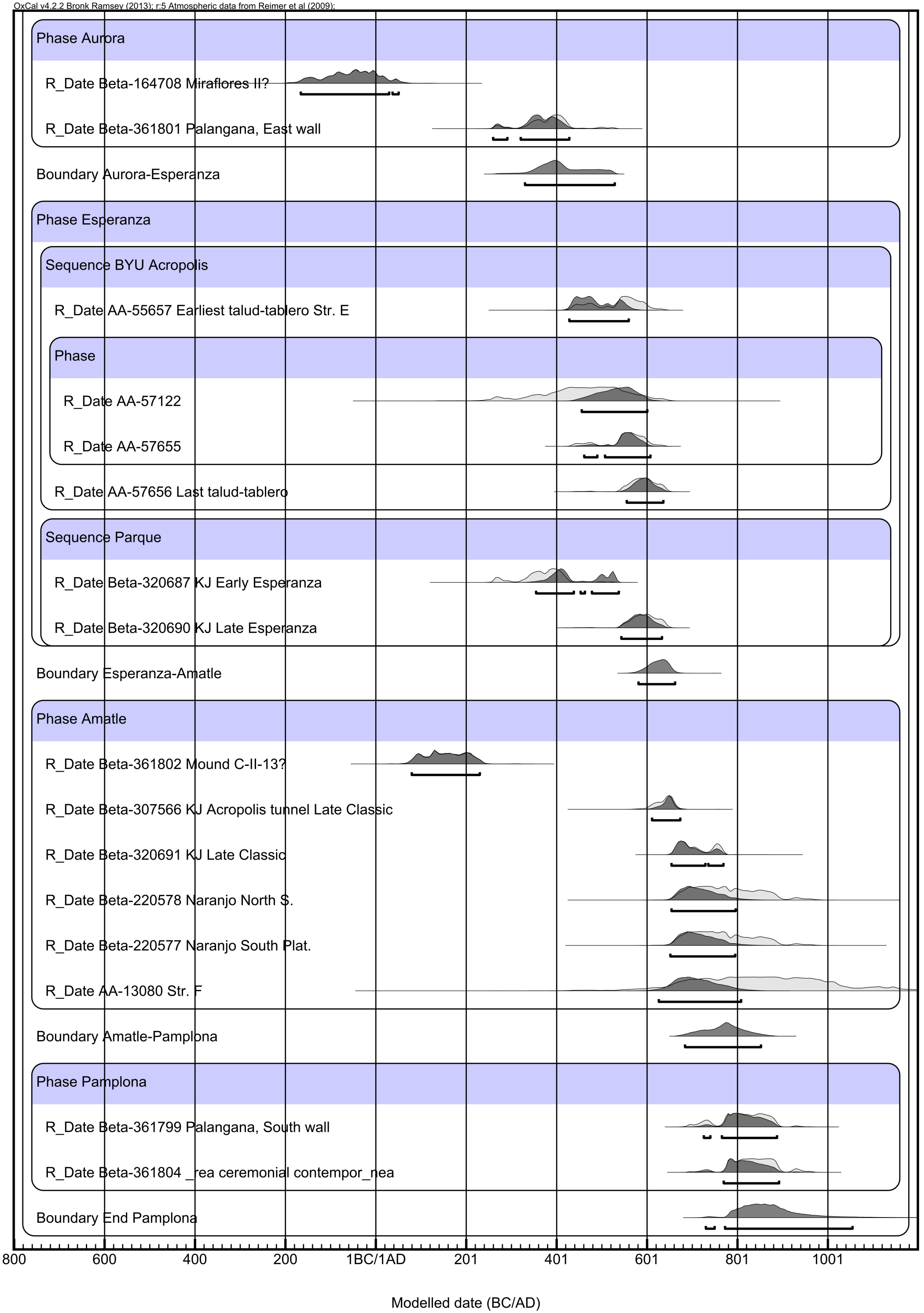

OxCal v4.2.2 Bronk Ramsey (2013); r:5 Atmospheric data from Reimer et al (2009);
Phase Aurora
R_Date Beta-164708 Miraflores II?
R_Date Beta-361801 Palangana, East wall
Boundary Aurora-Esperanza
Phase Esperanza
Sequence BYU Acropolis
R_Date AA-55657 Earliest talud-tablero Str. E
Phase
R_Date AA-57122
R_Date AA-57655
R_Date AA-57656 Last talud-tablero
Sequence Parque
R_Date Beta-320687 KJ Early Esperanza
R_Date Beta-320690 KJ Late Esperanza
Boundary Esperanza-Amatle
Phase Amatle
R_Date Beta-361802 Mound C-II-13?
R_Date Beta-307566 KJ Acropolis tunnel Late Classic
R_Date Beta-320691 KJ Late Classic
R_Date Beta-220578 Naranjo North S.
R_Date Beta-220577 Naranjo South Plat.
R_Date AA-13080 Str. F
Boundary Amatle-Pamplona
Phase Pamplona
R_Date Beta-361799 Palangana, South wall
R_Date Beta-361804 _rea ceremonial contempor_nea
Boundary End Pamplona
800
600
400
200
1BC/1AD
201
401
601
801
1001
Modelled date (BC/AD)

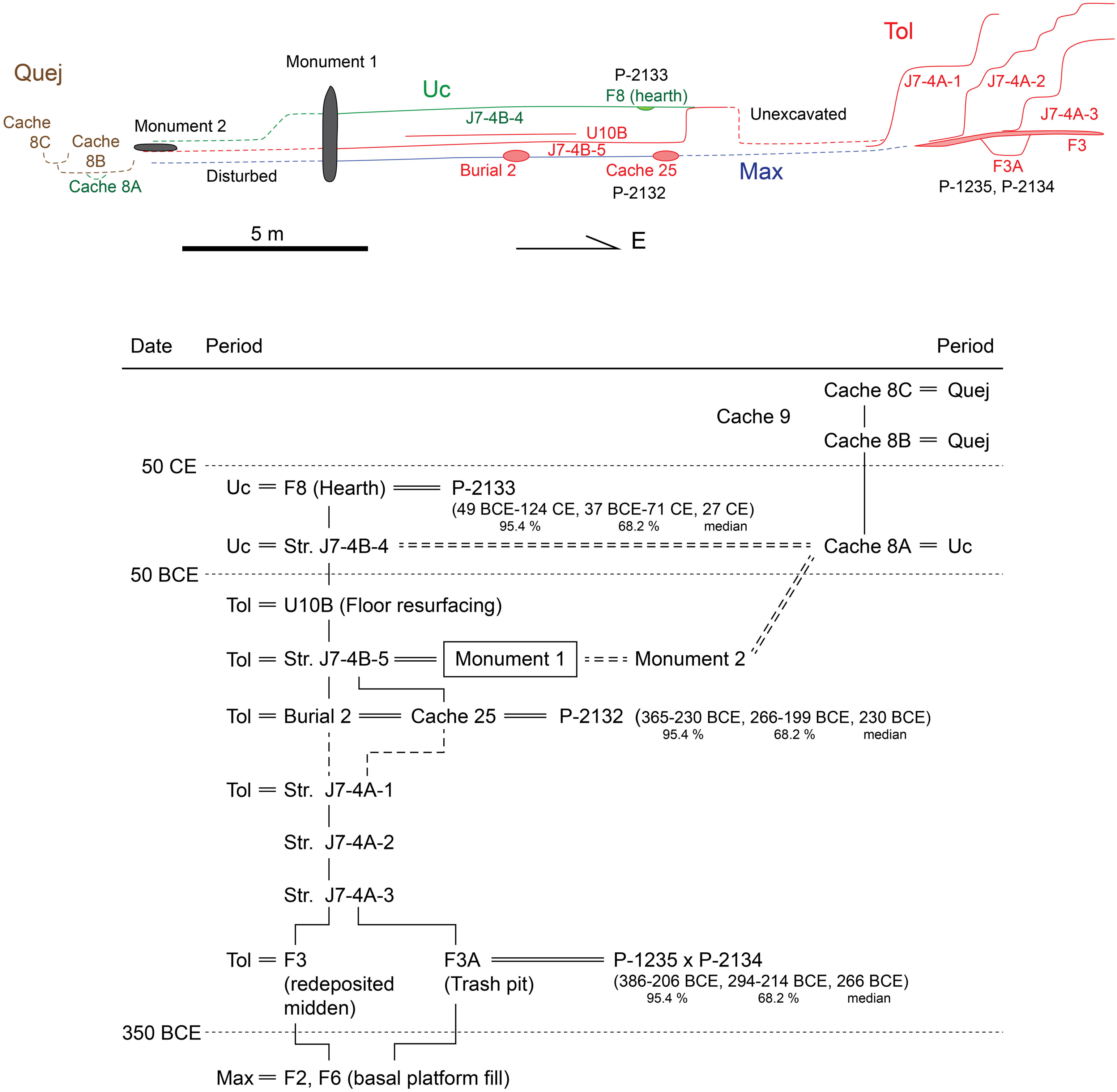

Quej
Cache 8C
Cache 8B
Cache 8A
Monument 2
Disturbed
Monument 1
Uc
J7-4B-4
P-2133
F8 (hearth)
U10B
J7-4B-5
Burial 2
Cache 25
P-2132
Unexcavated
Max
Tol
J7-4A-1
J7-4A-2
J7-4A-3
F3
F3A
P-1235, P-2134
5 m
E
Date
Period
Period
Cache 8C = Quej
Cache 9
Cache 8B = Quej
50 CE
Uc = F8 (Hearth) = P-2133
(49 BCE-124 CE, 37 BCE-71 CE, 27 CE)
95.4 % 68.2 % median
Uc = Str. J7-4B-4
Cache 8A = Uc
50 BCE
Tol = U10B (Floor resurfacing)
Tol = Str. J7-4B-5 = Monument 1 Monument 2
Tol = Burial 2 = Cache 25 = P-2132 (365-230 BCE, 266-199 BCE, 230 BCE)
95.4 % 68.2 % median
Tol = Str. J7-4A-1
Str. J7-4A-2
Str. J7-4A-3
Tol = F3
(redeposited
midden)
F3A
(Trash pit)
P-1235 x P-2134
(386-206 BCE, 294-214 BCE, 266 BCE)
95.4 % 68.2 % median
350 BCE
Max = F2, F6 (basal platform fill)

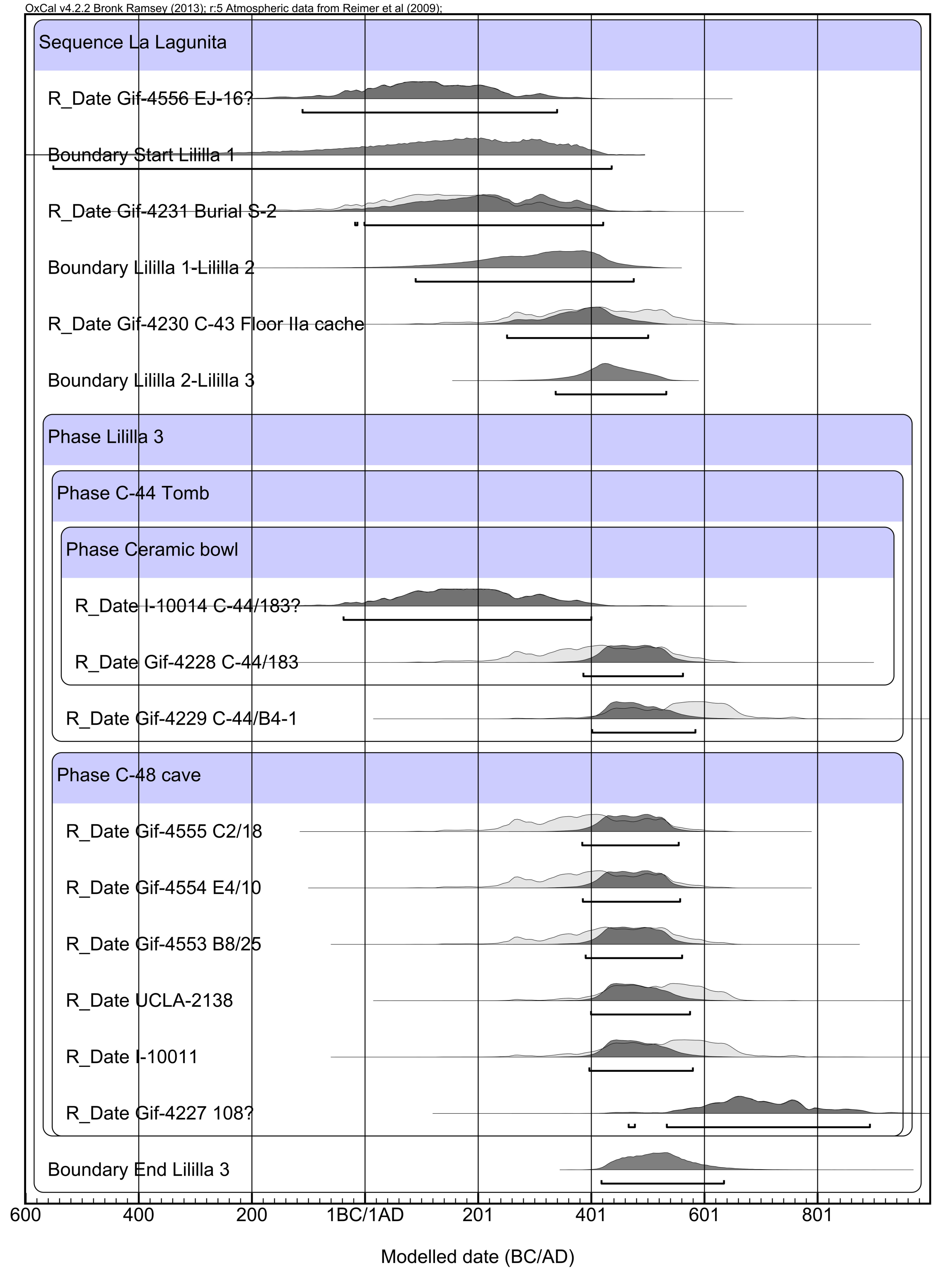
OxCal v4.2.2 Bronk Ramsey (2013); r:5 Atmospheric data from Reimer et al (2009);
Sequence La Lagunita
R_Date Gif-4556 EJ-16?
Boundary Start Lililla 1
R_Date Gif-4231 Burial S-2
Boundary Lililla 1-Lililla 2
R_Date Gif-4230 C-43 Floor IIa cache
Boundary Lililla 2-Lililla 3
Phase Lililla 3
Phase C-44 Tomb
Phase Ceramic bowl
R_Date I-10014 C-44/183?
R_Date Gif-4228 C-44/183
R_Date Gif-4229 C-44/B4-1
Phase C-48 cave
R_Date Gif-4555 C2/18
R_Date Gif-4554 E4/10
R_Date Gif-4553 B8/25
R_Date UCLA-2138
R_Date I-10011
R_Date Gif-4227 108?
Boundary End Lililla 3
600
400
200
1BC/1AD
201
401
601
801
Modelled date (BC/AD)

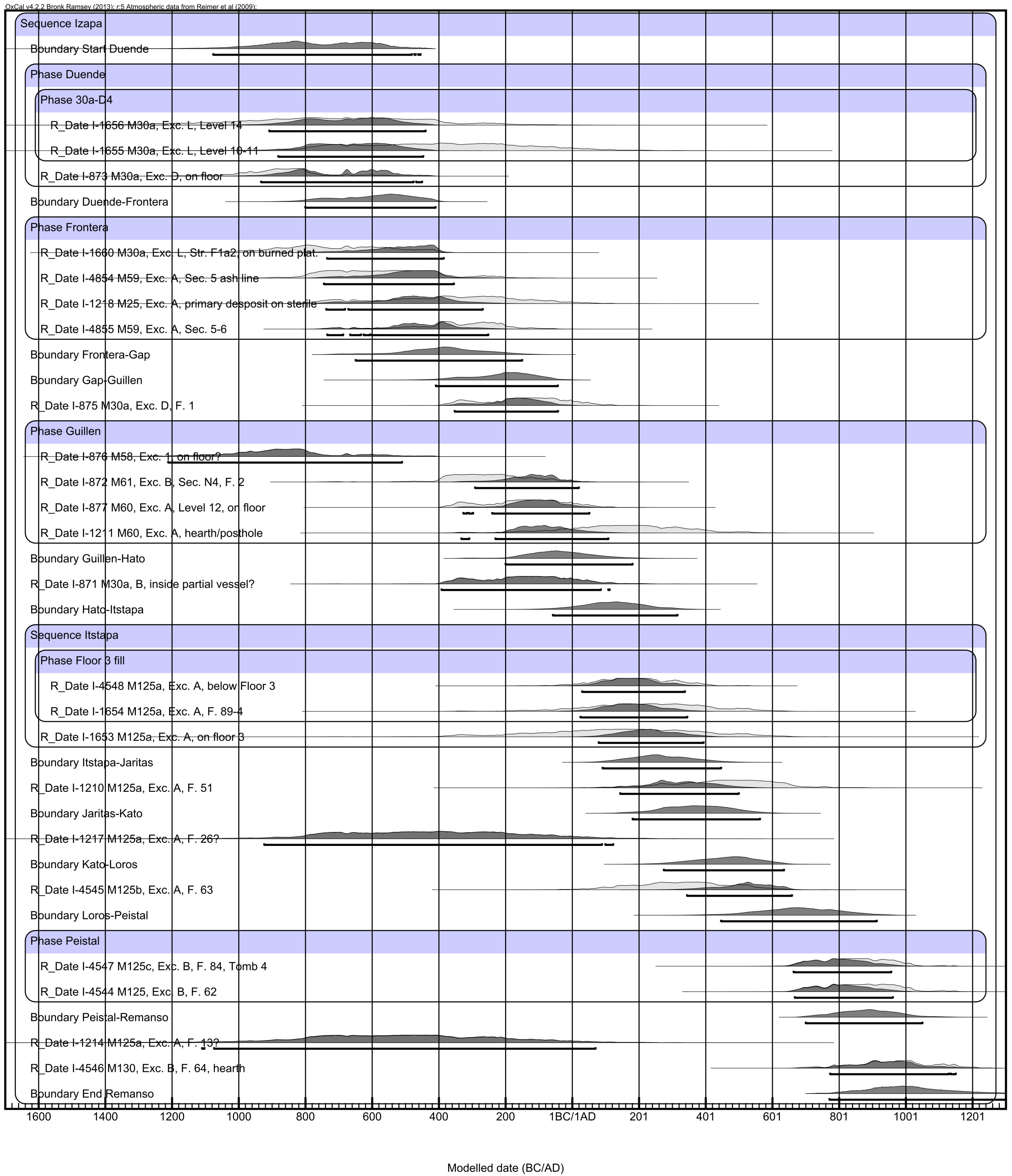
OxCal v4.2.2 Bronk Ramsey (2013); r:5 Atmospheric data from Reimer et al (2009);
Sequence Izapa
Boundary Start Duende
Phase Duende
Phase 30a-D4
R_Date I-1656 M30a, Exc. L, Level 14
R_Date I-1655 M30a, Exc. L, Level 10-11
R_Date I-873 M30a, Exc. D, on floor
Boundary Duende-Frontera
Phase Frontera
R_Date I-1660 M30a, Exc. L, Str. F1a2, on burned plat.
R_Date I-4854 M59, Exc. A, Sec. 5 ash line
R_Date I-1218 M25, Exc. A, primary desposit on sterile
R_Date I-4855 M59, Exc. A, Sec. 5-6
Boundary Frontera-Gap
Boundary Gap-Guillen
R_Date I-875 M30a, Exc. D, F. 1
Phase Guillen
R_Date I-876 M58, Exc. 1, on floor?
R_Date I-872 M61, Exc. B, Sec. N4, F. 2
R_Date I-877 M60, Exc. A, Level 12, on floor
R_Date I-1211 M60, Exc. A, hearth/posthole
Boundary Guillen-Hato
R_Date I-871 M30a, B, inside partial vessel?
Boundary Hato-Itstapa
Sequence Itstapa
Phase Floor 3 fill
R_Date I-4548 M125a, Exc. A, below Floor 3
R_Date I-1654 M125a, Exc. A, F. 89-4
R_Date I-1653 M125a, Exc. A, on floor 3
Boundary Itstapa-Jaritas
R_Date I-1210 M125a, Exc. A, F. 51
Boundary Jaritas-Kato
R_Date I-1217 M125a, Exc. A, F. 26?
Boundary Kato-Loros
R_Date I-4545 M125b, Exc. A, F. 63
Boundary Loros-Peistal
Phase Peistal
R_Date I-4547 M125c, Exc. B, F. 84, Tomb 4
R_Date I-4544 M125, Exc. B, F. 62
Boundary Peistal-Remanso
R_Date I-1214 M125a, Exc. A, F. 13?
R_Date I-4546 M130, Exc. B, F. 64, hearth
Boundary End Remanso
1600
1400
1200
1000
800
600
400
200
1BC/1AD
201
401
601
801
1001
1201
Modelled date (BC/AD)

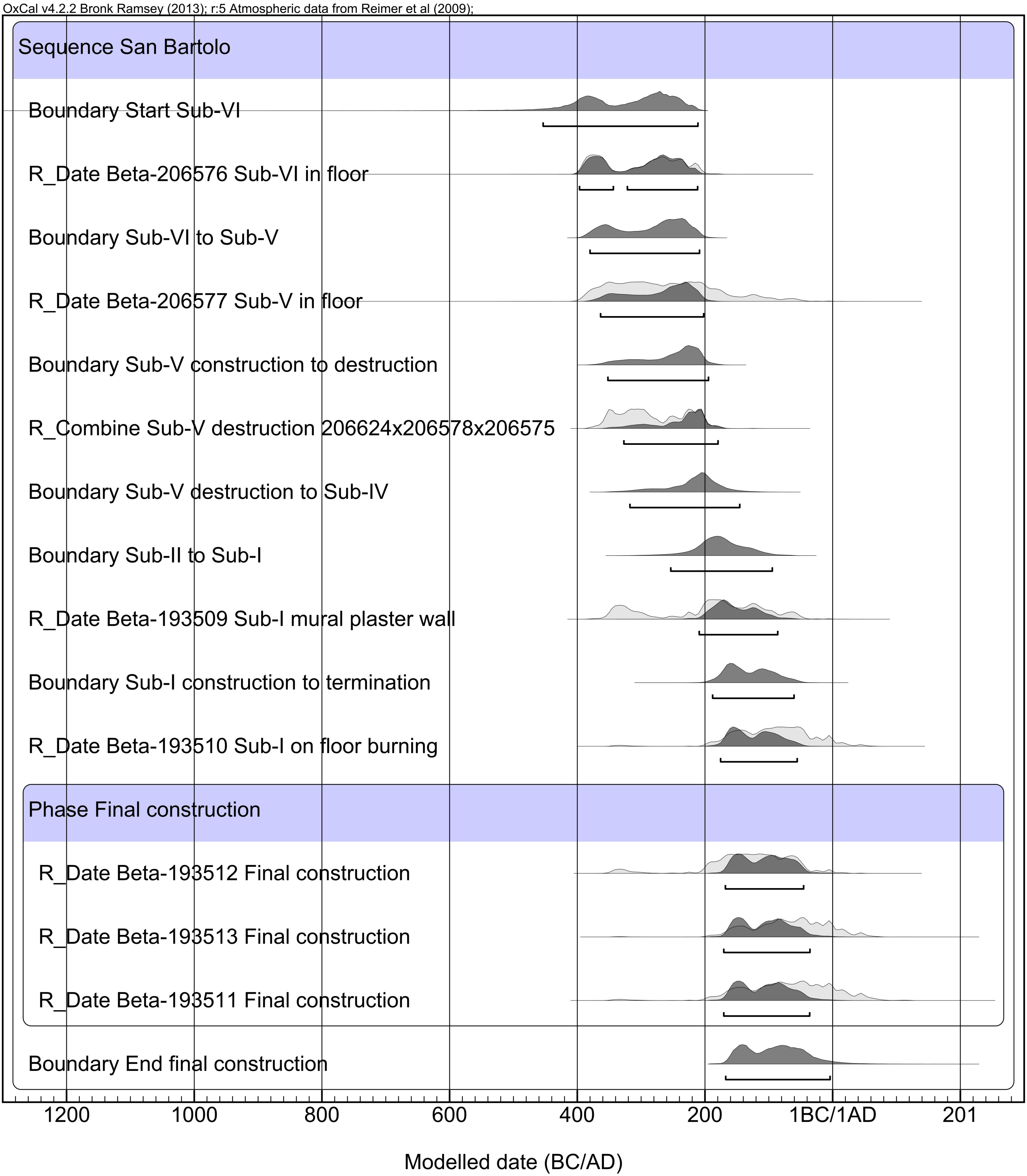
OxCal v4.2.2 Bronk Ramsey (2013); r:5 Atmospheric data from Reimer et al (2009);
Sequence San Bartolo
Boundary Start Sub-VI
R_Date Beta-206576 Sub-VI in floor
Boundary Sub-VI to Sub-V
R_Date Beta-206577 Sub-V in floor
Boundary Sub-V construction to destruction
R_Combine Sub-V destruction 206624x206578x206575
Boundary Sub-V destruction to Sub-IV
Boundary Sub-II to Sub-I
R_Date Beta-193509 Sub-I mural plaster wall
Boundary Sub-I construction to termination
R_Date Beta-193510 Sub-I on floor burning
Phase Final construction
R_Date Beta-193512 Final construction
R_Date Beta-193513 Final construction
R_Date Beta-193511 Final construction
Boundary End final construction
1200
1000
800
600
400
200
1BC/1AD
201
Modelled date (BC/AD)

## Supplemental Table 1. Radiocarbon dates from Kaminaljuyú and other regions.

| Lab code | Context | Ceramic phase | Radiocarbon date (B.P.) | 2σ calibrated date range | Source |
|---|---|---|---|---|---|
| **Kaminaljuyú Carnegie Project** | | | | | |
| Y-401 | C-III-10 2nd Str. | Arévalo | 2240±60 | 404 B.C.–166 B.C. | Deevey et al. 1959 |
| Y-402 | C-III-10 sandy layer over sterile | Arévalo | 2070±50 | 339 B.C.–A.D. 51 | Deevey et al. 1959 |
| Y-384 | Finca Las Charcas | Late Las Charcas | 2340±50 | 736 B.C.–211 B.C. | Deevey et al. 1959 |
| M-1257 | Finca Las Charcas | Late Las Charcas | 2280±130 | 762 B.C.–48 B.C. | Crane and Griffin 1964 |
| C-886 | C-III-6 same as Y-390 | Majadas | 2970±200 | 1691 B.C.–786 B.C. | Libby 1954 |
| Y-390 | C-III-6 Intrusive pit | Majadas | 2335±50 | 732 B.C.–210 B.C. | Deevey et al. 1959 |
| C-879 | D-III-10 same as Y-370 | Providencia | 3130±300 | 2278 B.C.–599 B.C. | Libby 1954 |
| Y-374 | Zacat, Sacatepéquez, Pit R 3 | Providencia | 2120±60 | 360 B.C.–A.D. 2 | Deevey et al. 1959 |
| Y-370 | D-III-10 older construction | Providencia | 1850±60 | A.D. 25–A.D. 332 | Deevey et al. 1959 |
| C-884 | E-III-3 same as Y-382 | Verbena | 3142±240 | 2010 B.C.–826 B.C. | Libby 1954 |
| C-887 | E-III-3 same as Y-391 | Verbena | 2490±300 | 1386 B.C.–A.D. 66 | Libby 1954 |
| Y-391 | E-III-3 Str. 5 fill | Verbena | 2025±60 | 197 B.C.–A.D. 85 | Deevey et al. 1959 |
| Y-377 | E-III-3 Tomb 1 | Verbena | 1940±60 | 88 B.C.–A.D. 230 | Deevey et al. 1959 |
| Y-382 | E-III-3 Str. 3b, 3c, 3d, 4 fill | Verbena | 1920±60 | 43 B.C.–A.D. 232 | Deevey et al. 1959 |
| Y-406 | D-III-1, midden sealed by terrace fill | Santa Clara | 1800±60 | A.D. 81–A.D. 382 | Deevey et al. 1959 |
| Y-396 | D-III-13 Post hole str. Floors 2 and 3 | Aurora | 1860±60 | A.D. 20–A.D. 325 | Deevey et al. 1959 |
| Y-378 | D-III-13 | Aurora | 1785±60 | A.D. 86–A.D. 392 | Deevey et al. 1959 |
| Y-405 | D-III-13 adobe str fill below Str. K | Aurora | 1660±60 | A.D. 249–A.D. 538 | Deevey et al. 1959 |
| Y-629 | D-III-13 below burial above stone | Aurora | 1560±70 | A.D. 349–A.D. 641 | Deevey et al. 1959 |
| **Kaminaljuyú Pennsylvania State University Project** | | | | | |
| I-6250 | 46-23-268 Level 15 | Providencia | 2355±90 | 766 B.C.–206 B.C. | Michels 1973 |
| I-6610 | 46-33-056 E-IV-6? Level 6 | Providencia | 2215±90 | 486 B.C.–1 B.C. | Michels 1973 |
| I-6384 | 46-12-396 Level 10 | Providencia | 2205±180 | 769 B.C.–A.D. 125 | Michels 1973 |
| I-6247 | 46-23-184 Level 14 | Providencia? | 1865±150 | 336 B.C.–A.D. 534 | Michels 1973 |
| I-6249 | 46-23-185 Level 12 | Verbena | 2090±90 | 367 B.C.–A.D. 69 | Michels 1973 |
| I-6305 | 46-23-072 Level 17 | Verbena | 2060±90 | 360 B.C.–A.D. 124 | Michels 1973 |
| I-6248 | 46-12-189 Level 6 | Arenal | 1965±90 | 197 B.C.–A.D. 242 | Michels 1973 |
| I-6332 | 46-23-023 Level 10 | Arenal | 1830±90 | 18 B.C.–A.D. 407 | Michels 1973 |
| I-6269 | 46-32-094 B-V-7 Level 10 | Aurora | 1915±90 | 160 B.C.–A.D. 327 | Michels 1973 |
| I-6308 | 46-23-072 Level 5 | Esperanza | 1750±90 | A.D. 71–A.D. 532 | Michels 1973 |
| I-6270 | 46-32-141 B-V-4 F. 4 | Amatle | 1225±90 | A.D. 655–A.D. 984 | Michels 1973 |
| **San Andrés Semetabaj** | | | | | |
| GX-5859 | Pit 2 plaza fill | Providencia | 2660±175 | 1268 B.C.–395 B.C. | Shook et al. 1979 |
| GX-5858 | Pit 7 plaza fill | Verbena-Arenal? | 1960±135 | 358 B.C.–A.D. 376 | Shook et al. 1979 |
| GX-5857 | Burned main post, upper platform | Verbena-Arenal? | 1865±130 | 192 B.C.–A.D. 431 | Shook et al. 1979 |
| GX-5856 | Burned main post, lower platform | Verbena-Arenal? | 1840±120 | 158 B.C.–A.D. 504 | Shook et al. 1979 |
| GX-5860 | Pit 4, intrusive pit | Early Classic | 1485±140 | A.D. 240–A.D. 863 | Shook et al. 1979 |

| | | | | | |
|---|---|---|---|---|---|
| **Kaminaljuyú Museum of Tobacco and Salt Project** | | | | | |
| GaK-17928 | D-III-1 on Str. 5 floor | Providencia | 2930±90 | 1390 B.C.–916 B.C. | Ohi 1994 |
| GaK-17124 | Burned Str. | Providencia | 2330±160 | 801 B.C.–46 B.C. | Ohi 1994 |
| GaK-17129 | Burned Str. | Providencia | 2210±120 | 732 B.C.–A.D. 53 | Ohi 1994 |
| NUTA-2110 | Burned Str. | Providencia | 2140±130 | 510 B.C.–A.D. 131 | Ohi 1994 |
| GaK-17925 | Under Floor 4 Offering 62 | End of Providencia | 2270±200 | 814 B.C.–A.D. 124 | Ohi 1994 |
| GaK-17128 | On Floor 4 Offering 16 | End of Verbena | 3750±300 | 3011 B.C.–1434 B.C. | Ohi 1994 |
| GaK-17125 | On Floor 4 Offering 23 | End of Verbena | 3000±110 | 1493 B.C.–930 B.C. | Ohi 1994 |
| GaK-17126 | On Floor 4 Offering 17 | End of Verbena | 2970±90 | 1416 B.C.–938 B.C. | Ohi 1994 |
| GaK-17123 | On Floor 4 Offering 19 | End of Verbena | 2540±90 | 831 B.C.–407 B.C. | Ohi 1994 |
| GaK-17127 | On Floor 4 Offering 26 | End of Verbena | 2070±130 | 394 B.C.–A.D. 212 | Ohi 1994 |
| NUTA-2084 | On Floor 4 Offering 57 | End of Verbena | 2060±180 | 536 B.C.–A.D. 382 | Ohi 1994 |
| NUTA-2109 | On Floor 4 Offering 24 | End of Verbena | 1950±130 | 354 B.C.–A.D. 381 | Ohi 1994 |
| NUTA-2056 | On Floor 4 Offering 29 | End of Verbena | 1920±160 | 360 B.C.–A.D. 424 | Ohi 1994 |
| GaK-17926 | On Floor 3 | Arenal | 2200±70 | 396 B.C.–60 B.C. | Ohi 1994 |
| GaK-17927 | D-III-1 on Str. 4 floor | Verbena-Arenal | 2060±80 | 357 B.C.–A.D. 120 | Ohi 1994 |
| **Urías, Antigua Valley** | | | | | |
| Beta-154187 | Subop 8 Nivel 25 | Sterile | 2810±40 | 1110 B.C.–843 B.C. | Robinson et al. 2006 |
| Beta-114963 | Subop 6 Nivel 24 | Las Charcas | 3260±120 | 1879 B.C.–1269 B.C. | Robinson et al. 2006 |
| Beta-114962 | Subop 2 Nivel 21 midden | Las Charcas | 2460±60 | 767 B.C.–408 B.C. | Robinson et al. 2006 |
| Beta-141169 | Subop 7 Nivel 21 | Las Charcas | 2370±50 | 751 B.C.–366 B.C. | Robinson et al. 2006 |
| Beta-141168 | Subop 8 Nivel 19 midden? | Las Charcas | 2570±100 | 897 B.C.–411 B.C. | Robinson et al. 2006 |
| Beta-114966 | Subop 2 Nivel 18 midden | Las Charcas | 2510±60 | 796 B.C.–416 B.C. | Robinson et al. 2006 |
| Beta-114961 | Subop 3 Nivel 18 | Las Charcas | 2380±60 | 756 B.C.–375 B.C. | Robinson et al. 2006 |
| Beta-114960 | Subop 3 Nivel 17 stela | Las Charcas | 2430±60 | 761 B.C.–400 B.C. | Robinson et al. 2006 |
| Beta-141170 | Subop 7 Nivel 16 burial | Las Charcas | 2250±50 | 398 B.C.–202 B.C. | Robinson et al. 2006 |
| **Naranjo, Santa Isabel, Kaminaljuyú Park, BYU Project** | | | | | |
| Beta-214075 | Naranjo Mon. 3 | Early Las Charcas | 2550±40 | 806 B.C.–540 B.C. | Arroyo 2010 |
| Beta-215654 | Naranjo N. Sec. | Early Las Charcas | 2550±40 | 806 B.C.–540 B.C. | Arroyo 2010 |
| Beta-215653 | Naranjo S Plat. | Early Las Charcas | 2500±40 | 791 B.C.–418 B.C. | Arroyo 2010 |
| Beta-220576 | Naranjo Mound 1 | Early Las Charcas | 2430±40 | 753 B.C.–402 B.C. | Arroyo 2010 |
| Beta-209872 | Naranjo N. Plat. | Early-Late Las Charcas transition | 2590±60 | 896 B.C.–523 B.C. | Arroyo 2010 |
| Beta-215655 | Naranjo Mon. 22 | Late Las Charcas | 2510±40 | 795 B.C.–421 B.C. | Arroyo 2010 |
| Beta-217153 | Naranjo SW S. | Late Las Charcas | 2270±40 | 401 B.C.–206 B.C. | Arroyo 2010 |
| Beta-307568 | Santa Isabel | Late Las Charcas | 2450±30 | 753 B.C.–410 B.C. | [a] |
| Beta-307569 | Santa Isabel | Late Las Charcas | 2410±30 | 741 B.C.–398 B.C. | [a] |
| Beta-164710 | KJ MII 3B-33 Lote 14 | Providencia | 2060±60 | 346 B.C.–A.D. 69 | Kaplan per. com. 2014[b] |
| Beta-361803 | KJ Mound E-III-5 | Verbena | 1990±30 | 49 B.C.–A.D. 74 | [a] |
| Beta-164706 | KJ MII 1B-4 Lote 14 | Verbena | 2020±40 | 161 B.C.–A.D. 68 | Kaplan per. com. 2014[b] |
| Beta-320689 | KJ Palangana south wall initial deposit | Arenal | 2120±30 | 346 B.C.–A.D. 49 | [a] |
| Beta-320688 | KJ C-II-12 base Palangana dedicatory | Arenal | 2050±30 | 166 B.C.–A.D. 20 | [a] |
| Beta-307567 | KJ early deposit Acropolis | Arenal | 1960±30 | 40 B.C.–A.D. 121 | [a] |
| Beta-164707 | KJ MII 2A-39/42 Lote 3 | Arenal | 1180±60 | A.D. 690–A.D. 983 | Kaplan per. com. 2014[b] |
| Beta-307565 | KJ Acropolis End Arenal | Santa Clara | 1930±30 | A.D. 3–A.D. 131 | [a] |

| | | | | | |
|---|---|---|---|---|---|
| Beta-361798 | KJ Palangana West wall | Santa Clara | 1820±30 | A.D. 91–A.D. 318 | [a] |
| Beta-361800 | KJ Palangana West wall | Santa Clara | 1790±30 | A.D. 132–A.D. 331 | [a] |
| Beta-164709 | KJ MII 3B-28 Lote 11 | Santa Clara | 2140±40 | 357 B.C.–50 B.C. | Kaplan per. com. 2014[b] |
| Beta-361801 | KJ Palangana, East wall | Aurora | 1660±30 | A.D. 259–A.D. 529 | [a] |
| Beta-164708 | KJ MII 3B-29 Lote 8 | Aurora | 2040±40 | 168 B.C.–A.D. 52 | Kaplan per. com. 2014[b] |
| Beta-320687 | KJ Park | Early Esperanza | 1670±30 | A.D. 258–A.D. 430 | [a] |
| AA-57122 | KJ BYU Acropolis | Esperanza | 1590±80 | A.D. 258–A.D. 623 | Houston et al. 2005 |
| AA-55657 | KJ Earliest talud-t. Str. E, BYU Acropolis | Esperanza | 1520±35 | A.D. 432–A.D. 611 | Houston et al. 2005 |
| AA-57655 | KJ BYU Acropolis | Esperanza | 1510±30 | A.D. 435–A.D. 623 | Houston et al. 2005 |
| AA-57656 | Last talud-tablero, BYU Acropolis | Esperanza | 1475±30 | A.D. 543–A.D. 644 | Houston et al. 2005 |
| Beta-320690 | KJ Park | Late Esperanza | 1470±30 | A.D. 545–A.D. 645 | [a] |
| Beta-361802 | KJ Mound C-II-13 | Amatle | 1860±30 | A.D. 80–A.D. 231 | [a] |
| Beta-307566 | KJ Acropolis tunnel Late Classic | Amatle | 1400±30 | A.D. 597–A.D. 670 | [a] |
| Beta-320691 | KJ Late Classic | Amatle | 1310±30 | A.D. 656–A.D. 773 | [a] |
| Beta-220577 | Naranjo South Plat. | Amatle | 1260±60 | A.D. 656–A.D. 891 | Arroyo 2010 |
| Beta-220578 | Naranjo North S. | Amatle | 1250±60 | A.D. 657–A.D. 935 | Arroyo 2010 |
| AA-13080 | KJ Str. F, BYU Acropolis | Amatle | 1180±150 | A.D. 589–A.D. 1162 | Houston et al. 2005 |
| Beta-361799 | KJ Palangana, South wall | Pamplona | 1210±30 | A.D. 694–A.D. 892 | [a] |
| Beta-361804 | KJ ceremonial area | Pamplona | 1190±30 | A.D. 720–A.D. 944 | [a] |
| **Chalchuapa and Santa Leticia** | | | | | |
| P-1551 | Chalchuapa | Tok | 2790±57 | 1113 B.C.–819 B.C. | Sharer 1978 |
| P-1807 | Chalchuapa | Colos | 2448±60 | 763 B.C.–405 B.C. | Sharer 1978 |
| P-1806 | Chalchuapa | Colos | 2385±63 | 761 B.C.–375 B.C. | Sharer 1978 |
| Q-3108 | Santa Leticia | Chul | 2320±100 | 763 B.C.–171 B.C. | Demarest 1986 |
| Q-3105 | Santa Leticia | Chul | 2090±85 | 362 B.C.–A.D. 65 | Demarest 1986 |
| Q-3101 | Santa Leticia | Chul | 2035±90 | 359 B.C.–A.D. 135 | Demarest 1986 |
| Q-3106 | Santa Leticia | Chul | 1940±90 | 174 B.C.–A.D. 316 | Demarest 1986 |
| P-1550 | Chalchuapa | Early Caynac | 2036±44 | 168 B.C.–A.D. 55 | Sharer 1978 |
| P-1805 | Chalchuapa | Early Caynac | 1965±61 | 157 B.C.–A.D. 211 | Sharer 1978 |
| Q-3109 | Santa Leticia | Early Caynac | 1930±90 | 169 B.C.–A.D. 321 | Demarest 1986 |
| Q-3104 | Santa Leticia | Early Caynac | 1930±80 | 161 B.C.–A.D. 254 | Demarest 1986 |
| Q-3102 | Santa Leticia | Early Caynac | 1870±65 | 18 B.C.–A.D. 326 | Demarest 1986 |
| Q-3103 | Santa Leticia | Early Caynac | 1775±85 | A.D. 53–A.D. 431 | Demarest 1986 |
| P-1547 | Chalchuapa | Late Caynac | 1817±38 | A.D. 86–A.D. 325 | Sharer 1978 |
| P-1803 | Chalchuapa | Vec | 1717±62 | A.D. 133–A.D. 505 | Sharer 1978 |
| **Salamá Valley** | | | | | |
| P-3208 | Sakajut | Early Xox | 2880±190 | 1605 B.C.–552 B.C. | Sharer and Sedat 1987 |
| P-2139 | Mangales D6-2 U1 | Max | 2290±50 | 484 B.C.–200 B.C. | Sharer and Sedat 1987 |
| P-2138 | El Portón C32 | Tol | 2320±50 | 706 B.C.–206 B.C. | Sharer and Sedat 1987 |
| P-2134 | El Portón F3A | Tol | 2300±50 | 508 B.C.–203 B.C. | Sharer and Sedat 1987 |
| P-2222 | Las Tunas C6-2 U11 | Tol | 2300±50 | 508 B.C.–203 B.C. | Sharer and Sedat 1987 |
| P-2132 | El Portón C25 | Tol | 2260±60 | 411 B.C.–168 B.C. | Sharer and Sedat 1987 |
| P-2135 | El Portón F3A | Tol | 2230±60 | 401 B.C.–119 B.C. | Sharer and Sedat 1987 |
| P-2137 | El Portón F21 | Tol | 2230±60 | 401 B.C.–119 B.C. | Sharer and Sedat 1987 |

| | | | | | |
|---|---|---|---|---|---|
| P-2220 | Las Tunas F2B | Tol | 2180±60 | 387 B.C.–61 B.C. | Sharer and Sedat 1987 |
| P-2136 | El Portón F19 | Tol | 2160±60 | 375 B.C.–53 B.C. | Sharer and Sedat 1987 |
| P-2219 | Las Tunas F3 | Tol | 2140±70 | 382 B.C.–2 B.C. | Sharer and Sedat 1987 |
| P-2221 | Las Tunas C6-2 F5 | Tol | 2020±60 | 191 B.C.–A.D. 119 | Sharer and Sedat 1987 |
| P-2133 | El Portón F8 | Uc | 1960±40 | 43 B.C.–A.D. 126 | Sharer and Sedat 1987 |
| **La Lagunita** | | | | | |
| Gif-4556 | La Lagunita, EJ-16 | Sterile | 1900±90 | 111 B.C.–A.D. 340 | Ichon and Viel 1984 |
| Gif-4231 | La Lagunita, Burial S-2 | Lilillá 1 | 1870±100 | 91 B.C.–A.D. 398 | Ichon and Viel 1984 |
| Gif-4230 | La Lagunita, C-43 Floor IIa cache | Lilillá 2 | 1640±90 | A.D. 176–A.D. 609 | Ichon and Viel 1984 |
| I-10014 | La Lagunita, C-44/183 | Lilillá 3 | 1840±95 | 39 B.C.–A.D. 401 | Ichon and Arnauld 1985 |
| Gif-4555 | La Lagunita, Cave C-48, C2/18 | Lilillá 3 | 1650±80 | A.D. 220–A.D. 592 | Ichon and Arnauld 1985 |
| Gif-4554 | La Lagunita, Cave C-48, E4/10 | Lilillá 3 | 1640±80 | A.D. 234–A.D. 595 | Ichon and Arnauld 1985 |
| Gif-4228 | La Lagunita, C-44/183 | Lilillá 3 | 1630±90 | A.D. 219–A.D. 618 | Ichon and Arnauld 1985 |
| Gif-4553 | La Lagunita Cave C-48, B8/25 | Lilillá 3 | 1610±80 | A.D. 253–A.D. 604 | Ichon and Arnauld 1985 |
| UCLA-2138 | La Lagunita, Cave C-48 | Lilillá 3 | 1530±80 | A.D. 353–A.D. 657 | Ichon and Arnauld 1985 |
| I-10011 | La Lagunita, Cave C-48 | Lilillá 3 | 1505±100 | A.D. 261–A.D. 760 | Ichon and Arnauld 1985 |
| Gif-4229 | La Lagunita, C-44/B4-1 | Lilillá 3 | 1480±90 | A.D. 382–A.D. 765 | Ichon and Arnauld 1985 |
| Gif-4227 | La Lagunita, Cave C-48, 108 | Lilillá 3 | 1350±90 | A.D. 470–A.D. 893 | Ichon and Arnauld 1985 |
| **Izapa** | | | | | |
| I-873 | M30a, Exc. D, on floor | Duende | 2695±100 | 1129 B.C.–541 B.C. | Lowe et al. 1982 |
| I-1656 | M30a, Exc. L, Level 14 | Duende | 2580±220 | 1306 B.C.–196 B.C. | Lowe et al. 1982 |
| I-1655 | M30a, Exc. L, Level 10-11 | Duende | 2310±210 | 897 B.C.–A.D. 84 | Lowe et al. 1982 |
| I-1660 | M30a, Exc. L, Str. F1a2, on burned plat. | Frontera? | 2600±130 | 1024 B.C.–398 B.C. | Lowe et al. 1982 |
| I-4854 | M59, Exc. A, Sec. 5 ash line | Frontera | 2440±130 | 832 B.C.–207 B.C. | Lowe et al. 1982 |
| I-4855 | M59, Exc. A, Sec. 5-6 | Frontera | 2280±90 | 747 B.C.–61 B.C. | Lowe et al. 1982 |
| I-1218 | M25, Exc. A, primary deposit on sterile | Frontera | 2280±150 | 779 B.C.–2 B.C. | Lowe et al. 1982 |
| I-875 | M30a, Exc. D, F. 1 | Frontera-Guillén transition | 2100±95 | 377 B.C.–A.D. 64 | Lowe et al. 1982 |
| I-876 | M58, Exc. 1, on floor | Early Guillén | 2695±120 | 1212 B.C.–511 B.C. | Lowe et al. 1982 |
| I-872 | M61, Exc. B, Sec. N4, F. 2 | Guillén | 2205±95 | 486 B.C.–A.D. 5 | Lowe et al. 1982 |
| I-877 | M60, Exc. A, Level 12, on floor | Guillén | 2100±90 | 372 B.C.–A.D. 59 | Lowe et al. 1982 |
| I-1211 | M60, Exc. A, hearth/posthole | Late Guillén | 1855±140 | 194 B.C.–A.D. 532 | Lowe et al. 1982 |
| I-871 | M30a, B, inside partial vessel | Hato | 2100±110 | 392 B.C.–A.D. 115 | Lowe et al. 1982 |
| I-1653 | M125a, Exc. A, on floor 3 | Itstapa | 1850±200 | 359 B.C.–A.D. 580 | Lowe et al. 1982 |
| I-4548 | M125a, Exc. A, below Floor 3 | Itstapa | 1830±95 | 37 B.C.–A.D. 409 | Lowe et al. 1982 |
| I-1654 | M125a, Exc. A, F. 89-4 | Itstapa | 1790±150 | 146 B.C.–A.D. 571 | Lowe et al. 1982 |
| I-1210 | M125a, Exc. A, F. 51 | Jaritas | 1565±145 | A.D. 129–A.D. 766 | Lowe et al. 1982 |
| I-1217 | M125a, Exc. A, F. 26 | Kato | 2330±220 | 926 B.C.–A.D. 123 | Lowe et al. 1982 |
| I-4545 | M125b, Exc. A, F. 63 | Loros | 1700±125 | A.D. 67–A.D. 601 | Lowe et al. 1982 |
| I-4547 | M125c, Exc. B, F. 84, Tomb 4 | Peistal | 1180±100 | A.D. 661–A.D. 1020 | Lowe et al. 1982 |
| I-4544 | M125, Exc. B, F. 62 | Peistal | 1155±100 | A.D. 660–A.D. 1035 | Lowe et al. 1982 |
| I-1214 | M125a, Exc. A, F. 13 | Remanso | 2400±235 | 1110 B.C.–A.D. 72 | Lowe et al. 1982 |
| I-4546 | M130, Exc. B, F. 64, hearth | Remanso | 1060±100 | A.D. 716–A.D. 1206 | Lowe et al. 1982 |
| **San Bartolo** | | | | | |

| | | | | | |
|---|---|---|---|---|---|
| Beta-206576 | Sub-VI in floor | Chicanel | 2260±40 | 398 B.C.–206 B.C. | Saturno et al. 2006 |
| Beta-206577 | Sub-V in floor | Chicanel | 2200±60 | 393 B.C.–108 B.C. | Saturno et al. 2006 |
| Beta-206624 | Sub-V destruction | Chicanel | 2260±40 | 398 B.C.–206 B.C. | Saturno et al. 2006 |
| Beta-206578 | Sub-V destruction | Chicanel | 2180±40 | 379 B.C.–114 B.C. | Saturno et al. 2006 |
| Beta-206575 | Sub-V destruction | Chicanel | 2150±40 | 359 B.C.–55 B.C. | Saturno et al. 2006 |
| Beta-193509 | Sub-I mural plaster wall | Chicanel | 2140±40 | 357 B.C.–50 B.C. | Saturno et al. 2006 |
| Beta-193510 | Sub-I on-floor burning | Chicanel | 2070±40 | 196 B.C.–A.D. 18 | Saturno et al. 2006 |
| Beta-193512 | Final construction | Chicanel | 2100±40 | 347 B.C.–2 B.C. | Saturno et al. 2006 |
| Beta-193511 | Final construction | Chicanel | 2050±50 | 192 B.C.–A.D. 55 | Saturno et al. 2006 |
| Beta-193513 | Final construction | Chicanel | 2050±40 | 174 B.C.–A.D. 50 | Saturno et al. 2006 |

*Note:* All samples are charcoal.

[a] Radiocarbon dates newly obtained by Arroyo, which have not been previously published. The measurements are corrected for isotopic fractionation.

[b] Jonathan Kaplan kindly provided these dates. To gain better information on the Kaminaljuyú chronology, Kaplan asked for charcoal samples collected during the Kaminaljuyú Miraflores II Project conducted by Juan Antonio Valdés and Marion Hatch in the 1990s. He did not publish these dates because he had not rechecked their contexts and associated materials. The measurements are corrected for isotopic fractionation.

**Supplemental Table 2. Ceramic cross-dating of Kaminaljuyú and relevant regions with diagnostic types and modes.**

| Type/mode | Upper Grijalva | Izapa | Tak'alik Ab'aj | La Lagunita | Ceibal/Maya Lowlands | Salamá | Kaminaljuyú | Chalchuapa |
|---|---|---|---|---|---|---|---|---|
| | **Kau** | **Itstapa** | **Alejos** | **Lililá 2** | **Xate 2** | | **Aurora** | **Vec** |
| Polychrome | Soyatitan | ? | ? | Ixcanrio | Ixcanrio | | Ixcanrio | No |
| | | | | **Lililá 1** | | | **Santa Clara** | **Late Caynac** |
| Large mammiform tetrapods | Yes | ? | Yes | Yes | Yes | | Yes | Yes |
| | **Ix** | **Hato** | **Ruth** | | | **Quej** | **Arenal** | |
| Large supports | Yes | Yes? | Yes | Yes | Yes | Yes | Yes | Yes |
| Kaminaljuyú Black-Brown post-slip fine incisions | Tabil | Yes | Yes | No | No | Canchon | Kaminaljuyú B. | Canchon |
| Verbena White | No | Yes | No | No | No | Chuacus? | Verbena W. | Pajonal |
| Arenante Coarse Incised | No | No? | No | No | No | No | Arenante | Conchalio |
| Iberia Orange | No | No? | No | No | Iberia | Chitucan | No | No |
| Wide horizontally everted effigy rim | San Jacinto | Yes | Yes | Yes | No | No | Yes | No |
| Wide horizontally everted rim | San Jacinto | Yes | Yes | Yes | No | No | Yes | No |
| | **Hun** | | **Rocío** | **Noguta 2** | **Xate 1** | **Uc** | **Verbena** | **Early Caynac** |
| Inner-prong censer | No?(Chiapa de Corzo[c]) | Yes | ? | No | No | ? | ? | ? |
| Izalco Usulután | No | No? | Izalco | ? | No | ? (Chicuxtin) | Izalco | Izalco |
| Pseudo-Usulután | Escobal | No? | No | Sacluc? | Sacluc/ Caramba | Caramba? | No | No |
| | | **Guillén** | | | | | | |
| Verbena White | No | No | No | No | No | No | Verbena W. | No? |
| Kaminaljuyú Black-Brown post-slip fine incisions | No | No | Yes | No | No (Tikal Burials 85 &167[b]) | Canchon | Kaminaljuyú B. | No |
| Kaminaljuyú Black-Brown post-slip coarse incisions | No | No | Yes? | Nogaro Variety C | No | Jorgia | Kaminaljuyú B. | Jorgia |
| Gancho rim | Yes | No | Yes | ? | Yes | Yes | Yes | Yes |
| Utatlán Red and Black Zoned Bichrome | No | No | No? | Utatlán | No | Utatlán | Utatlán | Olomega |
| Spiked censer | Yalmus | Yes | Yes | Yes? | Corriental | ? | No? | No |
| Inner-handle censer | No? | Yes | ? | No | No | Cotoxa | ? | Pululuya |
| | | | | | | **Tol** | | **Late Chul** |
| Conical supports | Yes | No? | Yes? | ? | Yes | ? | Yes | Yes |
| Nubbin supports | Yes | ? | Yes | ? | Yes | ? | Yes | Yes |
| Kaminaljuyú Black-Brown post-slip fine incisions | No | No | Yes | No | No | Yes | Kaminaljuyú B. | No |
| | **Guajil** | **Frontera** | **Nil** | **Noguta 1** | **Cantutse 2-3** | | **Providencia** | **Early Chul** |
| Inner-handle censer | No? | Yes | No? | No? | No? | No? | No? | No? |
| Utatlán Red and Black Zoned Bichrome | Utatlán | No | No? | Utatlán | No | No? | Utatlán | Olomega? |
| Scalloped ridge | No | No | Yes | Yes | No | Yes | Yes | Yes |
| Kaminaljuyú Black-Brown post-slip coarse incisions | No | No | Yes? | ? | No | Jorgia | Kaminaljuyú B. | Jorgia |
| Fine Red | Sierra | Mundet | Yes | Roqueño | Sierra | Xinacati | Rofino | Santa Tecla |

| | | | | | | | | |
|---|---|---|---|---|---|---|---|---|
| Purple on Fine Red | No | No | No? | No | No | Yes | Morfino | Santa Tecla |
| Red on Orange | No | No | No? | Otoño | No | Chisub | No | No |
| Labial-medial flange | Yes | No? | No? | ? | Yes | Yes | Yes | Yes |
| Orange Usulután | No | No | No? | Orfeo | No | Chopen | Verbena Red-Orange | Olocuitla |
| Thick cream Usulután | No | No | No? | No | No | Jicalapa | Usulután Cream Slipped | Jicalapa |
| Monte Alto Red jar | No | No | Monte Alto | No | No | No | Monte Alto | No |
| Xuc ware | No | No | Xuc | Trovador | No | No | Xuc | No |
| | **Foko** | | | **Santizo 2** | **Escoba 3-Cantutse 1** | | | |
| Labial-medial flange | Yes | No? | No? | No? | Yes | Yes | Yes | Yes |
| Graphite painted | No | No | No? | Stendal | No | Chahai | Morfino | Copinula |
| Wide horizontally everted rim | Yes | Yes | Yes | Yes | Yes | Yes | No | No |
| | | | | | | | **Late Las Charcas** | **Kal** |
| Glossy/Waxy red/orange | Mundet | Mundet | Naranja Glossy | Orfeo | Juventud/ Sierra | Xinacati | Yes | No |
| Glossy/Waxy cream | Teopisca | Teopisca | No? | Trovador | Pital/Flor | No | Morada | No |
| Glossy/Waxy black | Libertad | No | Negro Glossy | Nogaro | Chunhinta/ Polvero | Pinos: Guaxpac | Yes | No |
| Blochy orange resist | Nicapa | No | ? | Orfeo | Tierra Mojada | Chopen | Yes | Puxtla |
| | | | **Ixchiyá** | **Santizo 1** | **Escoba 2** | **Max** | | |
| Red on Buff Zoned Bichrome | No | Nasmin | ? | Bedelio | No | ? | Red on Buff | No |
| | **Enub** | **Escalón** | | | | | | |
| Glossy/Waxy red/orange | Kana | No | ? | Orfeo | Juventud | Chopen | Yes | No |
| Glossy/Waxy cream | No | No | ? | ? | Pital | No | Morada | No |
| Glossy/Waxy black | Libertad | No | ? | Nogaro | Chunhinta | Chimacho | Yes | No |
| Blotchy orange resist | Nicapa | Nicapa | ? | Orfeo | Tierra Mojada | Chopen | Yes | Puxtla |
| Pre-slip grooves | Yes | Yes | Yes? | Yes | Yes | Yes | Yes | Yes |
| Pallid/dusky red with post-slip incisions | No | No | ? | No | No | No | Pallid Red | Lolotique |
| Fine Orange | No | No | ? | No | Savana | No | No | Savana |
| Streaky Gray-Brown | No | No | ? | No | No | Choven | Streaky Gray-Brown | Jinuapa |
| Three-pronged censer | Yalmus | Yes? | ? | No? | No | Cotoxa | Yes | Cara Sucia |
| | **Dyosan** | **Duende** | | | **Escoba 1-Real 3** | **Late Xox** | **Early Las Charcas** | **Colos** |
| Pallid red with thick post-slip incisions | No | No | ? | | No | No | Pallid Red | Gualcho |
| Arevalo Red | No | No | ? | | No | Chirrum | Arevalo R. | No |
| Composite silhouette | No | Yes | Yes | | Yes | Yes | Yes | Yes |
| Chamfering | No | ? | Yes | | Yes | Yes | Yes | ? |
| Pre-slip grooves | Yes | ? | Yes? | | Yes | Yes | Yes | Yes |
| Zoned punctuation | No | No? | Yes | | No | Yes | Yes | Yes |
| Tubular spout | No | ? | ? | | Yes | ? | Yes? | Yes |
| Globular jars/bowls with tall tripods | No | ? | ? | | No | Beleju/Pachicaj | Yes | No |
| Dull-red bowl with applique fillets | No | ? | ? | | Yalmanchac | Chuachua | Red on Natural | No? |
| Outflared everted red rim with grooves | Dava | ? | ? | | Toribio | No | No | No |
| Small horizontally everted rim | Yes | ? | ? | | Yes | Yes? | Yes | Yes |
| | **Chacte** | | | | **Real 1-2** | | | **Late Tok** |

| | | | | | | | |
|---|---|---|---|---|---|---|---|
| Red rim and vertical line on cream/white | No | ? | ? | No (Tower Hill[a]) | No | Red on white | Ataco |
| Necked jar | Yes | Yes | Yes | Yes | Yes | Yes | Yes |
| Post-slip incisions | Yes | Yes | Yes | Yes | Yes | Yes | Yes |
| Pattern burnish | No | ? | ? | No (Patchchacan[a]) | El Congo | No | No |
| | **Jocote** | **Jocotal** | | | **Early Xox** | | **Early Tok** |
| Rocker stamping | No | ? | | | Beleju | | No? |
| Necked bowl | Yes? | Yes? | | | ? | | ? |
| Necked jar | No? | ? | | | ? | | ? |

[a] These types are not present at Ceibal but are reported from Cuello (Kosakowsky 1987).
[b] This type is not present at Ceibal or most lowland sites, but imported vessels of this type were found in Burials 85 and 167 at Tikal (Culbert 1993).
[c] This censer type is not reported from the Upper Grijalva River region but is present at Chiapa de Corzo (Lowe and Agrinier 1960).

| Years | | Kaminaljuyú | Uaxactún |
|---|---|---|---|
| 500 | | | |
| 400 | | Esperanza | Tzakol 3 |
| 300 | | | |
| 200 | | Salcaja | Tzakol 2 |
| 100 | | | Tzakol 1 |
| 1 | A.D. B.C. | Salcaja | (Holmul II) |
| 100 | | | |
| 200 | | Salcaja | Matzanel |
| 300 | | | (Holmul I) |
| 400 | | | |
| 500 | | Santa Clara | |
| 600 | | | |
| 700 | | | |
| 800 | | Arenal | |
| 900 | | | |
| 1000 | | | |
| 1100 | | | |
| 1200 | | Verbena | Chicanel |
| 1300 | | | |
| 1400 | | Providencia | |
| 1500 | | | |
| 1600 | | | |
| 1700 | | Sacatepéquez | |
| 1800 | | Mound C-III-6 | |
| 1900 | | | |
| 2000 | | | |
| 2100 | | | Mamom |
| 2200 | | | |
| 2300 | | | |
| 2400 | | | |
| 2500 | | Las Charcas | |
| 2600 | | | |
| 2700 | | | |
| 2800 | | | |
| 2900 | | | |
| 3000 | | | |

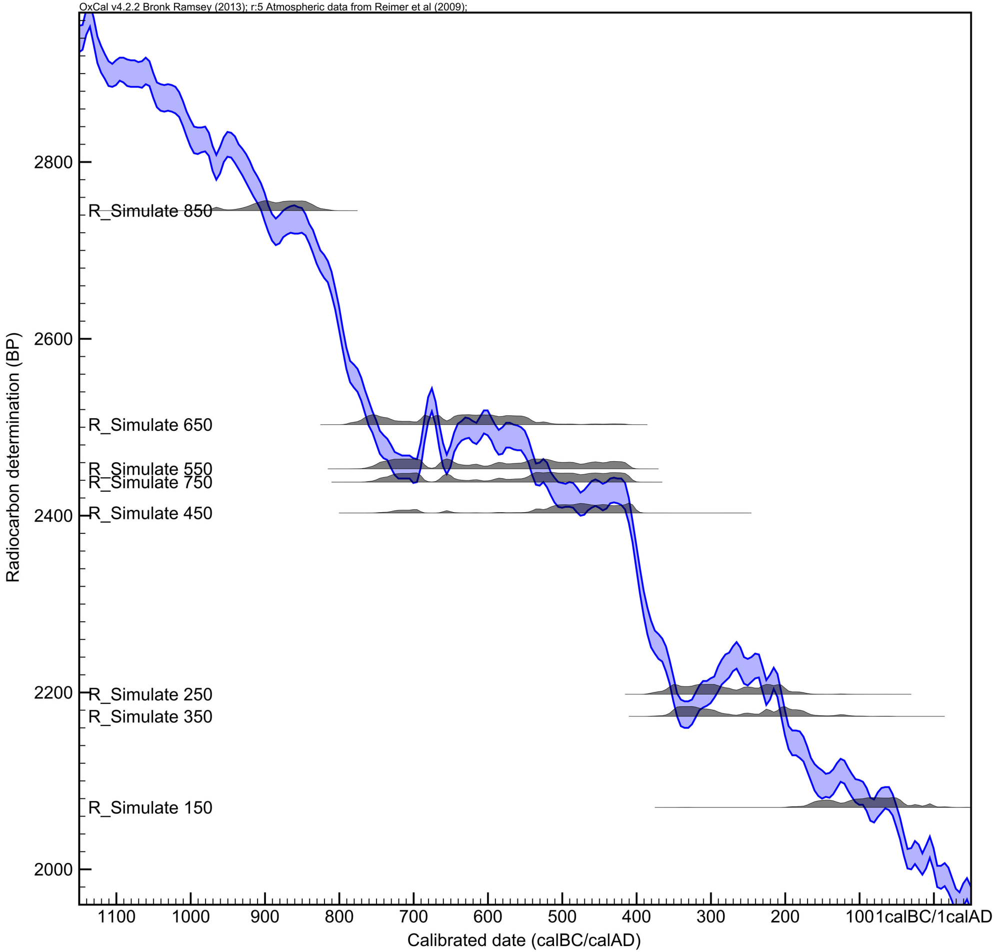
OxCal v4.2.2 Bronk Ramsey (2013); r:5 Atmospheric data from Reimer et al (2009);
R_Simulate 850
R_Simulate 650
R_Simulate 550
R_Simulate 750
R_Simulate 450
R_Simulate 250
R_Simulate 350
R_Simulate 150
2800
2600
2400
2200
2000
Radiocarbon determination (BP)
1100
1000
900
800
700
600
500
400
300
200
100
1calBC/1calAD
Calibrated date (calBC/calAD)

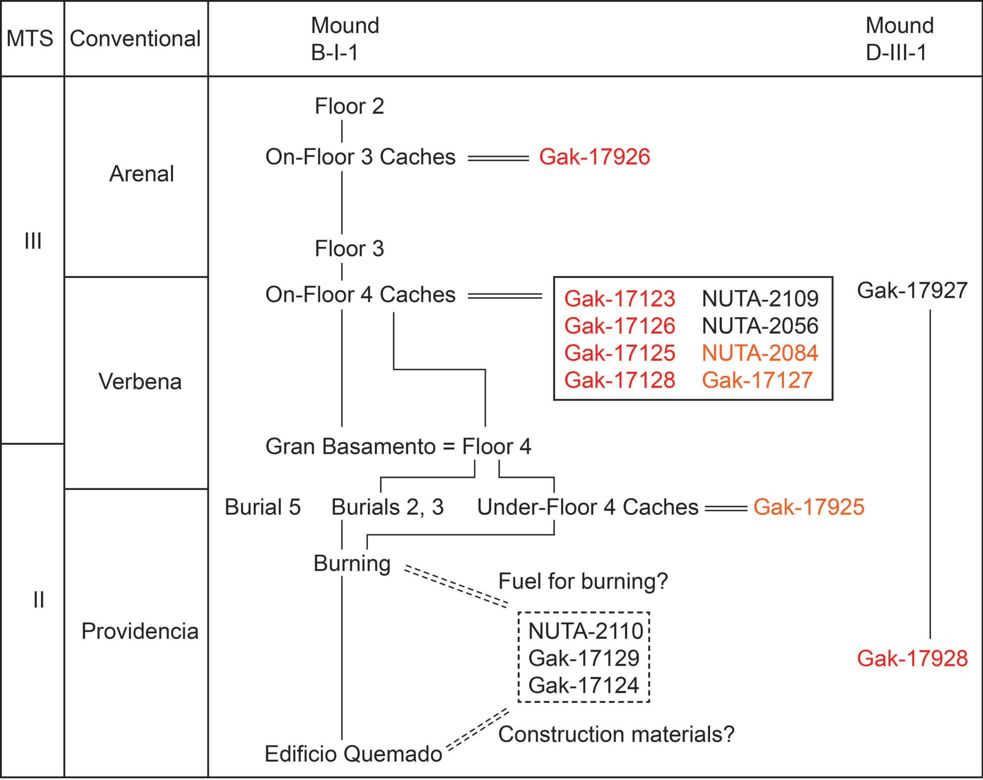


Gak-17928, etc. = outliers

Gak-17925, etc. = somewhat old wood?

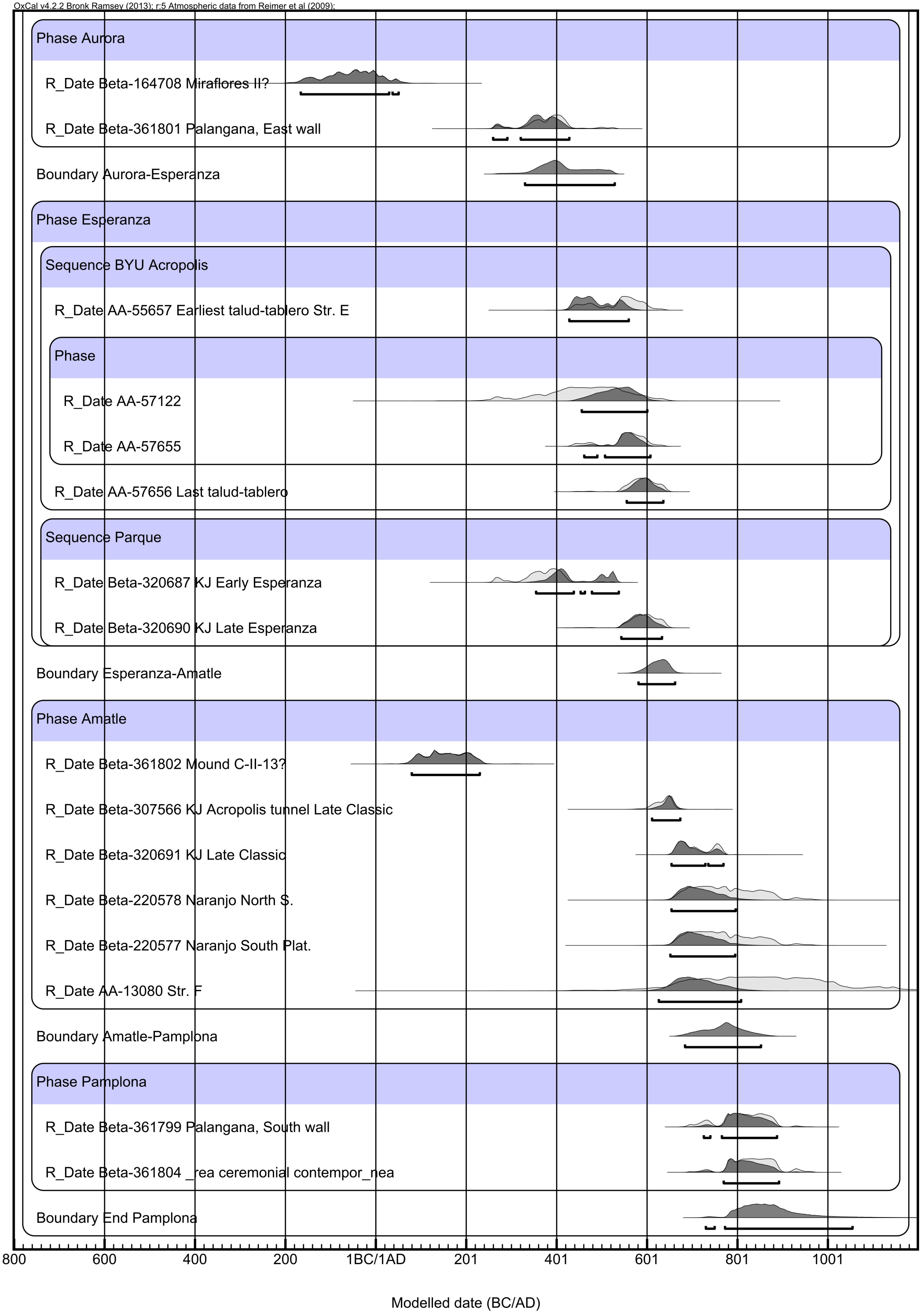
OxCal v4.2.2 Bronk Ramsey (2013); r:5 Atmospheric data from Reimer et al (2009);
Phase Aurora
R_Date Beta-164708 Miraflores II?
R_Date Beta-361801 Palangana, East wall
Boundary Aurora-Esperanza
Phase Esperanza
Sequence BYU Acropolis
R_Date AA-55657 Earliest talud-tablero Str. E
Phase
R_Date AA-57122
R_Date AA-57655
R_Date AA-57656 Last talud-tablero
Sequence Parque
R_Date Beta-320687 KJ Early Esperanza
R_Date Beta-320690 KJ Late Esperanza
Boundary Esperanza-Amatle
Phase Amatle
R_Date Beta-361802 Mound C-II-13?
R_Date Beta-307566 KJ Acropolis tunnel Late Classic
R_Date Beta-320691 KJ Late Classic
R_Date Beta-220578 Naranjo North S.
R_Date Beta-220577 Naranjo South Plat.
R_Date AA-13080 Str. F
Boundary Amatle-Pamplona
Phase Pamplona
R_Date Beta-361799 Palangana, South wall
R_Date Beta-361804 _rea ceremonial contempor_nea
Boundary End Pamplona
800
600
400
200
1BC/1AD
201
401
601
801
1001
Modelled date (BC/AD)

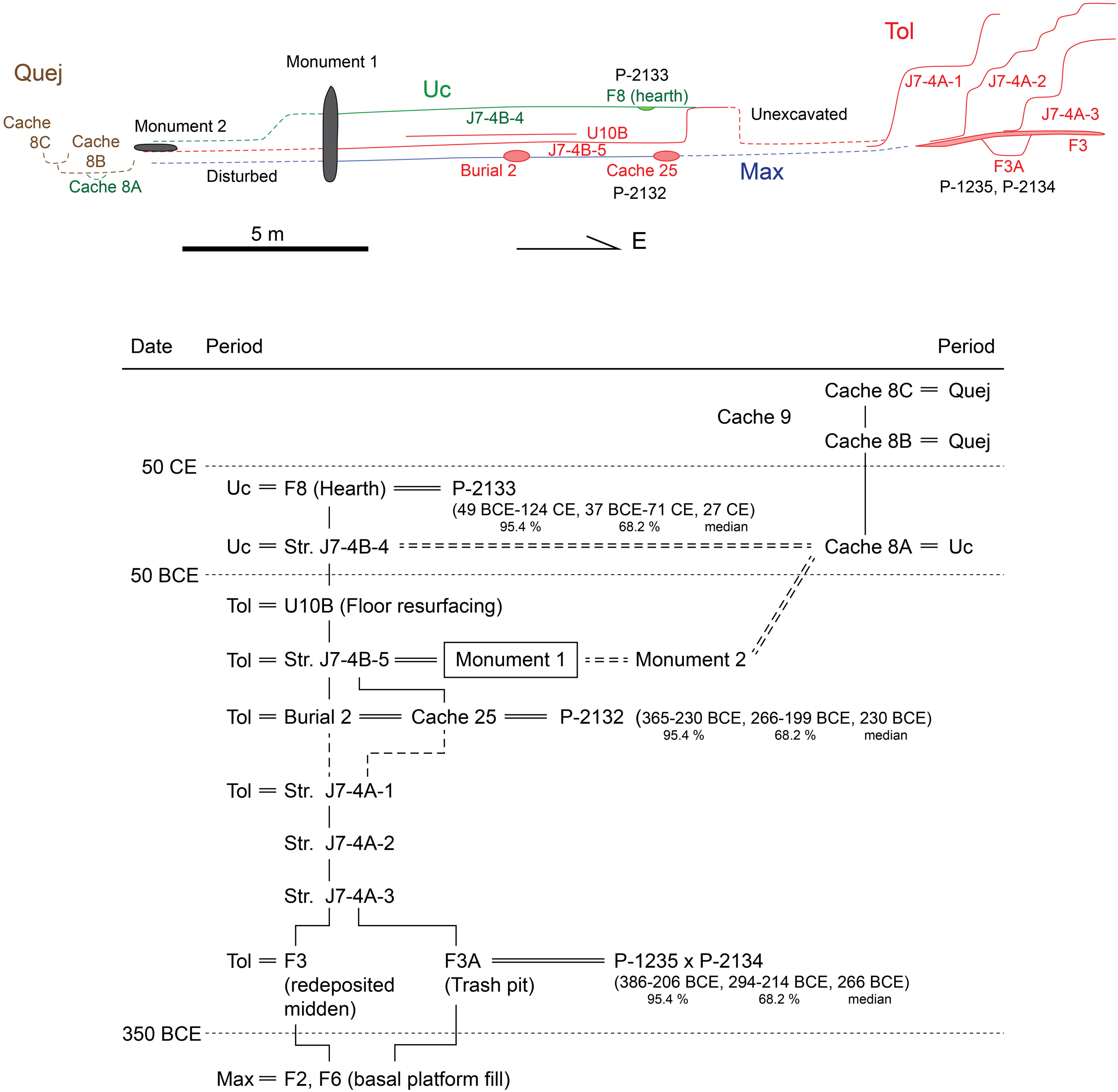

Quej
Cache 8C
Cache 8B
Cache 8A
Monument 2
Monument 1
Disturbed
Uc
J7-4B-4
P-2133
F8 (hearth)
U10B
J7-4B-5
Burial 2
Cache 25
P-2132
Unexcavated
Max
Tol
J7-4A-1
J7-4A-2
J7-4A-3
F3
F3A
P-1235, P-2134
5 m
E
Date
Period
Period
Cache 8C = Quej
Cache 9
Cache 8B = Quej
50 CE
Uc = F8 (Hearth) = P-2133
(49 BCE-124 CE, 37 BCE-71 CE, 27 CE)
95.4 % 68.2 % median
Uc = Str. J7-4B-4
Cache 8A = Uc
50 BCE
Tol = U10B (Floor resurfacing)
Tol = Str. J7-4B-5 = Monument 1 = Monument 2
Tol = Burial 2 = Cache 25 = P-2132 (365-230 BCE, 266-199 BCE, 230 BCE)
95.4 % 68.2 % median
Tol = Str. J7-4A-1
Str. J7-4A-2
Str. J7-4A-3
Tol = F3 (redeposited midden)
F3A (Trash pit) = P-1235 x P-2134
(386-206 BCE, 294-214 BCE, 266 BCE)
95.4 % 68.2 % median
350 BCE
Max = F2, F6 (basal platform fill)

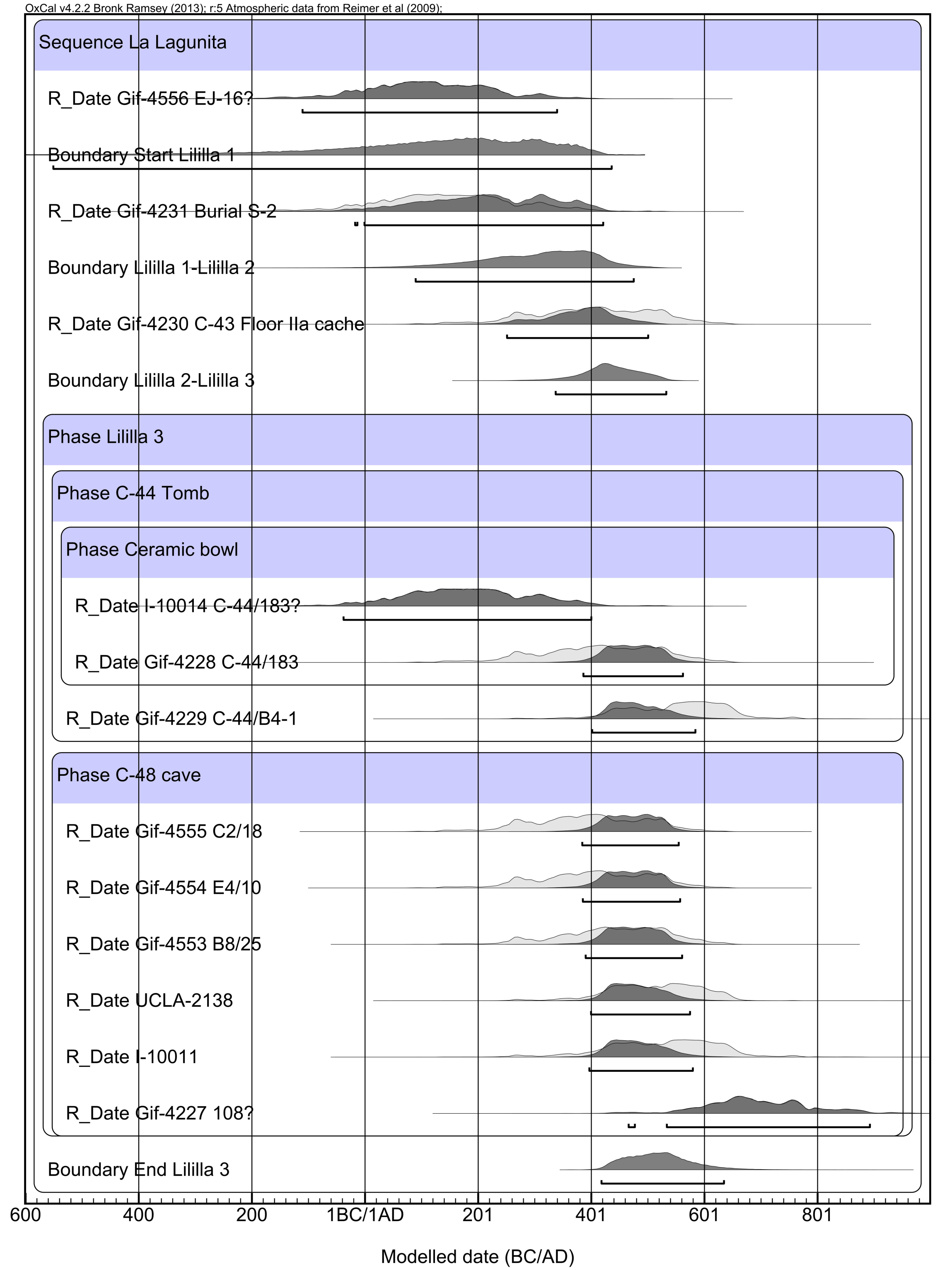

OxCal v4.2.2 Bronk Ramsey (2013); r:5 Atmospheric data from Reimer et al (2009);
Sequence La Lagunita
R_Date Gif-4556 EJ-16?
Boundary Start Lililla 1
R_Date Gif-4231 Burial S-2
Boundary Lililla 1-Lililla 2
R_Date Gif-4230 C-43 Floor IIa cache
Boundary Lililla 2-Lililla 3
Phase Lililla 3
Phase C-44 Tomb
Phase Ceramic bowl
R_Date I-10014 C-44/183?
R_Date Gif-4228 C-44/183
R_Date Gif-4229 C-44/B4-1
Phase C-48 cave
R_Date Gif-4555 C2/18
R_Date Gif-4554 E4/10
R_Date Gif-4553 B8/25
R_Date UCLA-2138
R_Date I-10011
R_Date Gif-4227 108?
Boundary End Lililla 3
600
400
200
1BC/1AD
201
401
601
801
Modelled date (BC/AD)

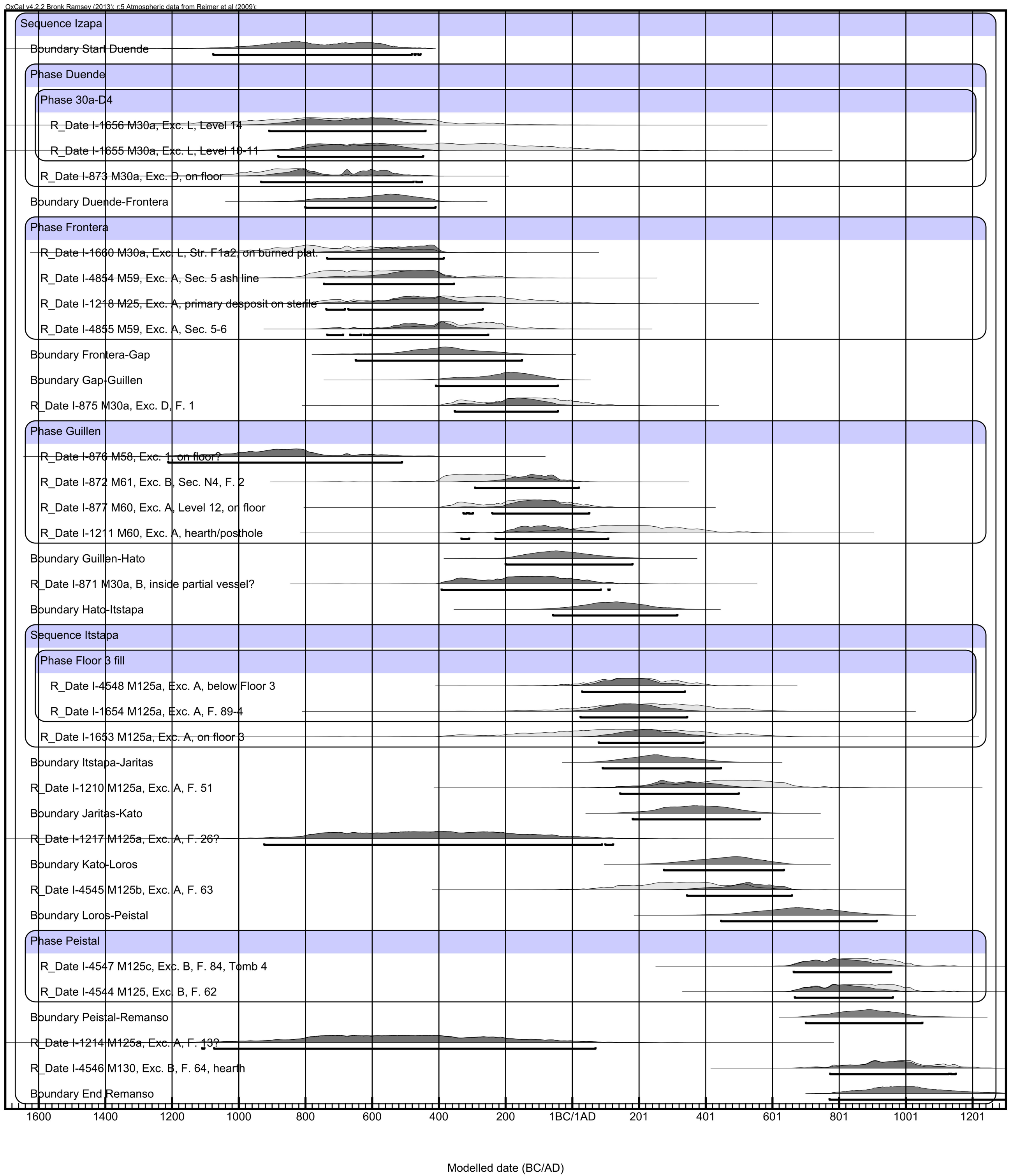

OxCal v4.2.2 Bronk Ramsey (2013); r:5 Atmospheric data from Reimer et al (2009);
Sequence Izapa
Boundary Start Duende
Phase Duende
Phase 30a-D4
R_Date I-1656 M30a, Exc. L, Level 14
R_Date I-1655 M30a, Exc. L, Level 10-11
R_Date I-873 M30a, Exc. D, on floor
Boundary Duende-Frontera
Phase Frontera
R_Date I-1660 M30a, Exc. L, Str. F1a2, on burned plat.
R_Date I-4854 M59, Exc. A, Sec. 5 ash line
R_Date I-1218 M25, Exc. A, primary desposit on sterile
R_Date I-4855 M59, Exc. A, Sec. 5-6
Boundary Frontera-Gap
Boundary Gap-Guillen
R_Date I-875 M30a, Exc. D, F. 1
Phase Guillen
R_Date I-876 M58, Exc. 1, on floor?
R_Date I-872 M61, Exc. B, Sec. N4, F. 2
R_Date I-877 M60, Exc. A, Level 12, on floor
R_Date I-1211 M60, Exc. A, hearth/posthole
Boundary Guillen-Hato
R_Date I-871 M30a, B, inside partial vessel?
Boundary Hato-Itstapa
Sequence Itstapa
Phase Floor 3 fill
R_Date I-4548 M125a, Exc. A, below Floor 3
R_Date I-1654 M125a, Exc. A, F. 89-4
R_Date I-1653 M125a, Exc. A, on floor 3
Boundary Itstapa-Jaritas
R_Date I-1210 M125a, Exc. A, F. 51
Boundary Jaritas-Kato
R_Date I-1217 M125a, Exc. A, F. 26?
Boundary Kato-Loros
R_Date I-4545 M125b, Exc. A, F. 63
Boundary Loros-Peistal
Phase Peistal
R_Date I-4547 M125c, Exc. B, F. 84, Tomb 4
R_Date I-4544 M125, Exc. B, F. 62
Boundary Peistal-Remanso
R_Date I-1214 M125a, Exc. A, F. 13?
R_Date I-4546 M130, Exc. B, F. 64, hearth
Boundary End Remanso
1600
1400
1200
1000
800
600
400
200
1BC/1AD
201
401
601
801
1001
1201
Modelled date (BC/AD)

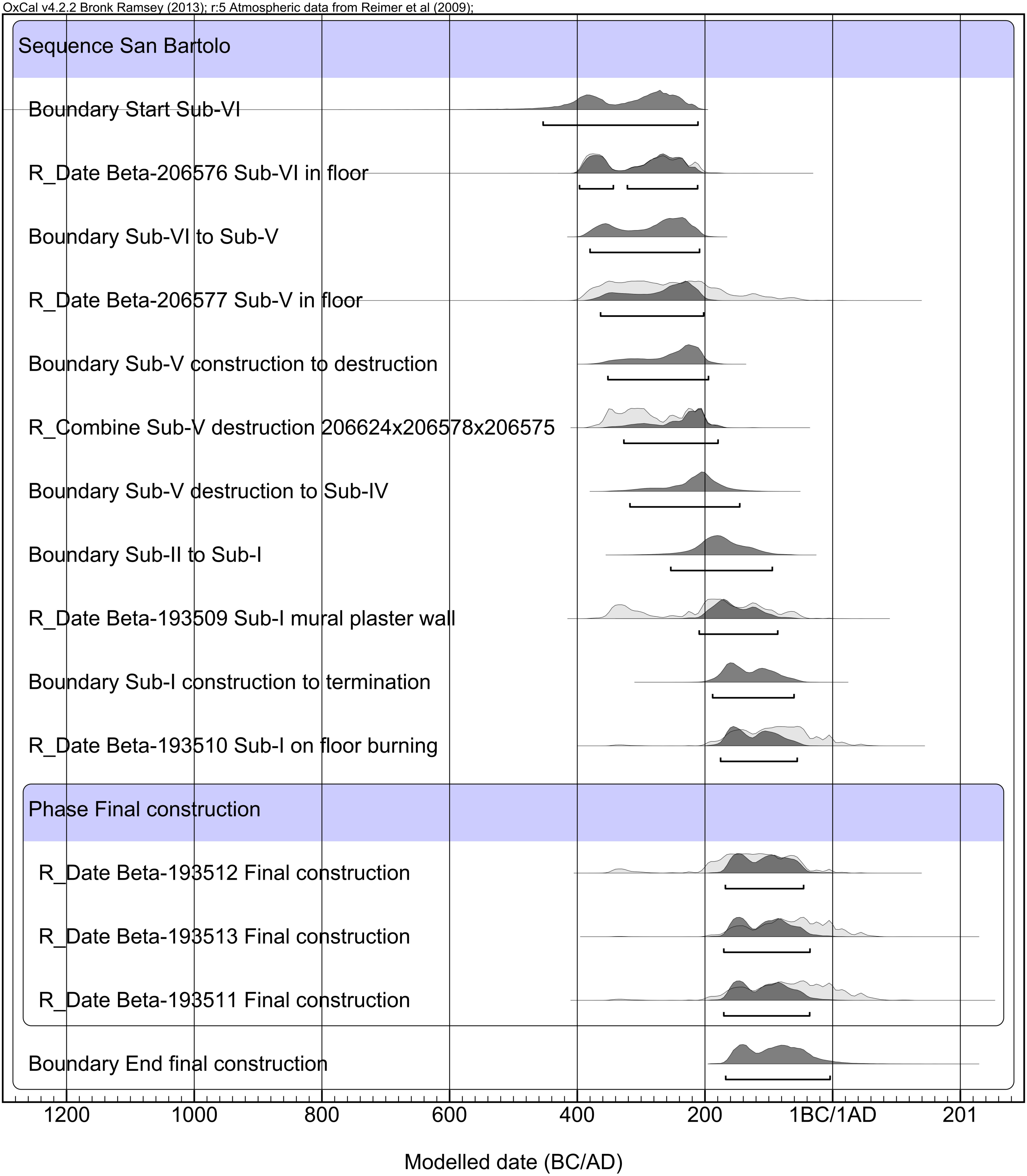

OxCal v4.2.2 Bronk Ramsey (2013); r:5 Atmospheric data from Reimer et al (2009);
Sequence San Bartolo
Boundary Start Sub-VI
R_Date Beta-206576 Sub-VI in floor
Boundary Sub-VI to Sub-V
R_Date Beta-206577 Sub-V in floor
Boundary Sub-V construction to destruction
R_Combine Sub-V destruction 206624x206578x206575
Boundary Sub-V destruction to Sub-IV
Boundary Sub-II to Sub-I
R_Date Beta-193509 Sub-I mural plaster wall
Boundary Sub-I construction to termination
R_Date Beta-193510 Sub-I on floor burning
Phase Final construction
R_Date Beta-193512 Final construction
R_Date Beta-193513 Final construction
R_Date Beta-193511 Final construction
Boundary End final construction
1200
1000
800
600
400
200
1BC/1AD
201
Modelled date (BC/AD)